

A Unified Near Infrared Spectral Classification Scheme for T Dwarfs

Adam J. Burgasser^{1,2,3}, T. R. Geballe⁴, S. K. Leggett⁵, J. Davy Kirkpatrick⁶ and David A. Golimowski⁷

ABSTRACT

A revised near infrared classification scheme for T dwarfs is presented, based on and superseding prior schemes developed by Burgasser et al. and Geballe et al., and defined following the precepts of the MK Process. Drawing from two large spectroscopic libraries of T dwarfs identified largely in the Sloan Digital Sky Survey and the Two Micron All Sky Survey, nine primary spectral standards and five alternate standards spanning spectral types T0 to T8 are identified that match criteria of spectral character, brightness, absence of a resolved companion and accessibility from both northern and southern hemispheres. The classification of T dwarfs is formally made by the direct comparison of near infrared spectral data of equivalent resolution to the spectra of these standards. Alternately, we have redefined five key spectral indices measuring the strengths of the major H₂O and CH₄ bands in the 1–2.5 μ m region that may be used as a proxy to direct spectral comparison. Two methods of determining T spectral type using these indices are outlined and yield equivalent results. These classifications are also equivalent to those from prior schemes, implying that no revision of existing spectral type trends is required. The one-dimensional scheme presented here provides a first step toward the observational characterization of the lowest luminosity brown dwarfs currently known. Future extensions to incorporate spectral variations arising from differences in photospheric dust content, gravity and metallicity are briefly discussed. A compendium of all currently known T dwarfs with updated classifications is presented.

¹Department of Astrophysics, Division of Physical Sciences, American Museum of Natural History, Central Park West at 79th Street, New York, NY 10024; adam@amnh.org

²Spitzer Fellow

³Now at Massachusetts Institute of Technology, Kavli Institute for Astrophysics and Space Research, Building 37, 77 Massachusetts Ave, Cambridge, MA 02139; ajb@mit.edu

⁴Gemini Observatory, 670 North A’ohoku Place, Hilo, HI 96720

⁵Joint Astronomy Centre, 660 North A’ohoku Place, Hilo, HI 96720

⁶Infrared Processing and Analysis Center, M/S 100-22, California Institute of Technology, Pasadena, CA 91125

⁷Department of Physics & Astronomy, Johns Hopkins University, 3701 San Martin Drive, Baltimore, MD 21218

Subject headings: stars: fundamental parameters — stars: low mass, brown dwarfs

1. Introduction

Classification is an important first step in all fields of empirical natural science, from biology (e.g., the taxonomy of species; Linnaeus 1735) to chemistry (e.g., the periodic table of elements; Mendeleev 1869) to several subfields of astronomy (e.g., the Hubble sequence of galaxies; Hubble 1936). The identification and quantification of similarities and differences in observed phenomena help to clarify their governing mechanisms, while providing a standard framework for our continually evolving theoretical understanding.

In stellar astronomy, spectral classification has been and remains a powerful tool, providing insight into the physical characteristics of stars and stellar populations and enabling the study of Galactic structure (e.g., Morgan, Sharpless & Osterbrock 1952). From the first stellar spectral groups designated by Secchi (1866), the classification of stars has evolved in complexity and breadth, largely due to advances in technology and the compilation of large spectral catalogs (e.g., the Henry Draper [HD] catalog, Cannon & Pickering 1918-1924). Nevertheless, nearly all existing stellar classification schemes remain observationally based. The most successful follow the MK Process (Morgan, Keenan & Kellman 1943; Morgan & Keenan 1973; Keenan & McNeil 1976; Morgan, Abt & Tapscott 1978; Garrison 1984; Corbally, Gray & Garrison 1994), a method by which stellar classes are defined by specific standard stars, and all other stars are classified by the direct comparison of spectra over a designated wavelength range and resolution. This method allows spectral classifications to remain independent of physical interpretations, concepts which can evolve even as the spectra themselves generally do not. Examples of MK classification schemes include the Michigan Catalogue of Spectral Types for the HD stars (Houk & Cowley 1975; Houk 1978, 1982; Houk & Smith-Moore 1988; Houk & Swift 1999), automated classifications through neural network techniques (e.g., von Hippel et al. 1994; Bailer-Jones et al. 1998) and classification schemes of normal stars at UV (e.g., Rountree & Sonneborn 1993) and near infrared (e.g., Wallace & Hinkle 1997) wavelengths.

Recently, two new spectral classes of low mass stars and brown dwarfs (stars with insufficient mass to sustain hydrogen fusion; Kumar 1962; Hayashi & Nakano 1963) have been identified. These sources, the L dwarfs (Kirkpatrick et al. 1999; Martín et al. 1999) and the T dwarfs (Burgasser et al. 2002a; Geballe et al. 2002, hereafter B02 and G02, respectively), lie beyond the standard stellar main sequence. L dwarfs exhibit optical spectra with waning TiO and VO bands (characteristic of M dwarfs); strengthening metal hydride, alkali and H₂O absorption features; and increasingly red optical/near infrared spectral energy distributions. T dwarfs (Figure 1) are distinguished by the presence of CH₄ absorption in their near infrared spectra, a species generally found in planetary atmospheres (Geballe et al. 1996); as well as pressure-broadened alkali resonance lines in the optical, strong H₂O bands, and collision induced H₂ absorption (Saumon et al. 1994; Borysow, Jørgensen, & Zheng 1997) suppressing flux at 2 μ m. The sequence of spectral types from M to L to T is

largely one of decreasing effective temperature and luminosity (Dahn et al. 2002; Vrba et al. 2004; Golimowski et al. 2004, however, see § 5.1), and as such is a natural extension of the stellar main sequence.

Initial spectral classification schemes for the colder of these two classes, the T dwarfs, have been proposed independently by B02 and G02. Both are defined in the 1–2.5 μm spectral window where T dwarfs emit the majority of their flux (e.g., Allard et al. 2001). The underlying philosophies of these two schemes are somewhat different, however. B02 identified seven representative standards spanning types T1 to T8 (excluding subtype T4), and classified a sizeable but inhomogeneous sample of low and moderate resolution spectra by the comparison of a set of spectral indices. G02 analyzed a smaller but homogenous sample of $\lambda/\Delta\lambda \sim 400$ near infrared spectra, and also determined classifications using spectral indices, but no standards were explicitly defined.

Neither of these schemes adhere rigorously to the MK Process; yet, despite their underlying differences, classifications differ by no more than 0.5 subtypes (Burgasser et al. 2003a). On the other hand, the existence of two separate classification schemes for T dwarfs has led to redundancies and confusion in the literature (e.g., Scholz et al. 2003). Furthermore, the relatively few T dwarfs (roughly 30) known at the time these schemes were introduced, and the limited observations available for them, resulted in an incomplete sampling of the T class and a potentially biased set of spectral standards (e.g, contaminated by peculiar sources and unresolved multiple systems). With over twice as many T dwarfs now known, primarily identified in the Sloan Digital Sky Survey (York et al. 2000, hereafter SDSS) and the Two Micron All Sky Survey (Cutri et al. 2003, hereafter 2MASS), and with extensive imaging, spectroscopic and astrometric data now available, it is an opportune time to revisit the classification of these cold brown dwarfs.

In this article, we present a revised near infrared spectral classification scheme for T dwarfs which unifies and supersedes the studies of B02 and G02. This scheme is defined by a set of carefully screened spectral standard stars spanning types T0 to T8, and is demonstrated on two distinct, large and homogenous spectral samples. In § 2 we describe the primary spectral libraries employed for this study, as well as additional published datasets examined. In § 3 we identify and give detailed information on the nine primary and five alternate spectral standards used to define the sequence. In § 4 we review the methods of classifying T dwarfs, focusing first on the direct comparison of spectral data to the standard spectra as dictated by the MK Process, then describing secondary methods based on redefined spectral indices sampling the major near infrared H_2O and CH_4 bands. In § 5 we discuss the revised subtypes, comparing them to prior classifications. We also discuss how extensions to this one-dimensional scheme may be made to account for secondary spectral variations, arising from physical differences in atmospheric dust content, surface gravity and metallicity; and speculate on the end of the T dwarf class. Individual sources are discussed in § 6. Results are summarized in § 7. We provide a compendium of all presently known T dwarfs and their revised spectral types in the Appendix.

2. Spectral Data

Defining the classification of a stellar class necessitates a sizeable set of homogeneous (similar resolution and wavelength coverage) spectra for both standards and classified sources. Our study draws primarily on two large, near infrared spectral libraries of T dwarfs obtained with the SpeX instrument (Rayner et al. 2003), mounted on the 3.0m NASA Infrared Telescope Facility Telescope; and the Cooled Grating Spectrometer 4 (Wright et al. 1993, hereafter CGS4), mounted on the 3.5m United Kingdom Infrared Telescope (UKIRT). These libraries are available in electronic form upon request.¹

The SpeX dataset is composed of prism-dispersed spectra covering 0.8-2.5 μm in a single order at a spectral resolution $\lambda/\Delta\lambda \approx 150$. These low resolution data sufficiently sample the broad H₂O and CH₄ bands present at near infrared wavelengths, but cannot resolve important line features such as the 1.25 μm K I doublets (Figure 1). The SpeX sample includes 59 spectra of 43 T dwarfs and two optically-classified L8 dwarfs (Kirkpatrick et al. 1999), a subset of which have been previously published (Burgasser et al. 2004a; Burgasser, Burrows & Kirkpatrick 2005; Cruz et al. 2004). All data have been homogeneously acquired and reduced using the Spextool package (Vacca et al. 2003; Cushing, Vacca & Rayner 2004).

The CGS4 dataset is composed of 41 spectra of 39 T dwarfs and two optically-classified L8 dwarfs, with typical resolutions $\lambda/\Delta\lambda \approx 300$ -500.² At these slightly higher resolutions, details within the molecular bands and atomic line absorptions can be resolved. The CGS4 spectra, nominally spanning 0.85-2.5 μm , require four instrumental settings to acquire, although some of the data encompass a subset of this spectral range. Nearly all of these spectra have been previously published (Geballe et al. 1996; Strauss et al. 1999; Leggett et al. 2000; Tsvetanov et al. 2000; Geballe et al. 2001, 2002; Knapp et al. 2004), and data acquisition and reduction procedures can be found in the literature.

In addition to these two primary datasets, we have examined other late-type L and T dwarf spectra reported in the literature (Oppenheimer et al. 1995; Cuby et al. 1999; Burgasser et al. 2000c, 2002c; Burgasser, McElwain, & Kirkpatrick 2003; Nakajima et al. 2001, 2004; Liu et al. 2002; Zapatero Osorio et al. 2002; McLean et al. 2003; McCaughrean et al. 2004; Cushing, Rayner & Vacca 2005). As these data have been obtained with assorted instrumentation, they vary in both spectral resolution and wavelength coverage. Details of all of the spectral datasets examined here are given in Table 1.

While many of the T dwarfs with near infrared spectral data have been observed by multiple instruments (e.g., 25 have been observed with both SpeX and CGS4), nearly all have had no more than two separate observations with a single instrument. The general absence of spectral monitoring

¹Also see <http://DwarfArchives.org> and <http://www.jach.hawaii.edu/~skl/LTdata.html>.

²With the exception of the bright T dwarf 2MASS 0559-1404, which was observed at twice this resolution (G02).

observations prevents a robust analysis of spectral variability for T dwarfs and its impact on their classification. We therefore assume that the spectra are effectively static and representative of each source over long periods.

3. Spectral Standards

3.1. Primary Standards

The selection of spectral standards is the most important aspect of defining a classification scheme, as these sources provide the framework for the entire class. The set of standards should encompass the full range of spectral morphologies observed while being sufficiently unique so as to be readily distinguishable. Peculiar (e.g., unusual metallicity) or highly variable standards are poor choices as they may improperly skew the sequence. A standard that is too difficult to observe — due to its faintness, unobservable declination or obscuration by a nearby bright star — is also of limited utility.

We have therefore attempted to select T dwarf spectral standards that conform to the following criteria:

- reasonably bright,
- not known to be spectroscopically peculiar (see § 6),
- not known to be a resolved multiple system and
- within 25° of the celestial equator.

We have considered both previously selected standards (B02) and more recently discovered sources for which extensive data (spectroscopic and otherwise) have been obtained. In this manner, nine primary standards spanning subtypes T0 through T8 that best represent the known population of T dwarfs were identified. Coordinates and photometric measurements are given in Table 2; additional data are provided in the Appendix. Detailed descriptions are as follows:

*SDSS 1207+0244*³ (T0): Recently identified in the SDSS by Knapp et al. (2004) and classified T0 on the G02 scheme, this source is favored over the bright, unequal-brightness binary SDSS 0423–0414AB (G02; Burgasser et al. 2005). No high resolution imaging or parallax observations have yet been made for this source.

³Source designations are abbreviated in the manner SDSS hhmm±ddmm, where the suffix conforms to IAU nomenclature convention and is the sexagesimal Right Ascension (hours and minutes) and declination (degrees and arcminutes) at J2000 equinox. Full designations are provided for all known T dwarfs in the Appendix.

SDSS 0837–0000 (T1): One of the first “L/T transition objects” discovered by Leggett et al. (2000), this source was the T1 spectral standard on the B02 scheme and classified T0.5 by G02. It is unresolved in *Hubble Space Telescope (HST)* observations (Burgasser et al. in prep.) and has a poorly constrained parallactic distance of 29 ± 12 pc (Vrba et al. 2004).

SDSS 1254–0122 (T2): Also identified by Leggett et al. (2000), this relatively bright source ($J = 14.66\pm 0.03$; Leggett et al. 2000⁴) was the T2 standard in the B02 scheme and classified likewise on the G02 scheme. It is a single source in *HST* images (Burgasser et al. in prep.). Three parallax distance measurements have been made for SDSS 1254–0122, one in the optical (11.8 ± 0.3 pc, Dahn et al. 2002) and two in the near infrared (13.7 ± 0.4 , Tinney et al. 2003; and 13.2 ± 0.5 pc, Vrba et al. 2004); note the disagreement. A more precise measure is expected from the USNO near infrared parallax program (F. Vrba 2005, priv. comm.).

2MASS 1209–1004 (T3): This recently discovered T dwarf (Burgasser et al. 2004a) replaces the apparent double SDSS 1021–0304AB (Burgasser et al. in prep.) as the T3 standard on the B02 system. No high resolution imaging or parallax measurements of this source have yet been obtained.

2MASS 2254+3123 (T4): While outside of our declination constraint, the spectrum of this relatively bright ($J = 15.01\pm 0.03$; Knapp et al. 2004) T dwarf fits ideally between those of our T3 and T5 standards. Identified by B02 and originally classified T5 on that scheme (Knapp et al. 2004 classify it T4 on the G02 scheme), it is unresolved in *HST* observations (Burgasser et al. in prep.). No parallax measurement has been reported for this source. Enoch, Brown & Burgasser (2003) report a marginally significant rise of 0.5 ± 0.2 mag in the *K*-band flux of this object over the course of three nights, but this possible detection of variability has yet to be confirmed.

2MASS 1503+2525 (T5): This bright source ($J = 13.55\pm 0.03$; Knapp et al. 2004) was identified by Burgasser et al. (2003c) and originally classified T5.5 on the B02 scheme. While at a slightly higher declination than our adopted selection criteria, the brightness of 2MASS 1503+2525 and lack of a visible companion (Burgasser et al. in prep.) make it an excellent choice as a spectral standard. No parallax distance measurement has been reported for this source.

SDSS 1624+0029 (T6): The first known field T dwarf, identified by Strauss et al. (1999) in the SDSS database and classified T6 on both the B02 and G02 schemes, SDSS 1624+0029 is a representative and easily accessible standard. It is unresolved in *HST* imaging observations (Burgasser et al. in prep.), and has a parallax distance measurement of 11.00 ± 0.15 pc (Tinney, Burgasser, & Kirkpatrick 2003, see also Dahn et al. 2002; Vrba et al. 2004). Nakajima et al. (2000) report very low levels (1-3%) of variability in fine H₂O features between 1.53 and 1.58 μm in the spectrum of the source, but not significant enough to affect its gross spectral morphology.

2MASS 0727+1710 (T7): Identified by B02 and selected as the T7 standard in that scheme (Knapp

⁴Near infrared photometry reported in the text are generally based on the Mauna Kea Observatory (MKO) filter system (Simons & Tokunaga 2002; Tokunaga, Simons & Vacca 2002), unless otherwise specified (e.g., Table 14).

et al. 2004 classify it T8 on the G02 scheme), this source remains an excellent spectral standard. No high resolution imaging observations have been reported for 2MASS 0727+1710, but it has a parallax distance measurement of 9.09 ± 0.17 pc (Vrba et al. 2004).

2MASS 0415–0935 (T8): The coldest ($T_{eff} \approx 700$ K; Vrba et al. 2004; Golimowski et al. 2004) and latest-type T dwarf known, this source was initially identified by B02 and selected as the T8 standard in that scheme. It is the sole T9 on the G02 system (Knapp et al. 2004). 2MASS 0415–0935 is unresolved in *HST* imaging observations (Burgasser et al. in prep.), and is the closest (isolated) field T dwarf to the Sun currently known, with a parallax distance measurement of 5.75 ± 0.10 pc (Vrba et al. 2004).

Figure 2 displays the spectral sequence of these standards, along with the L8 optical standard 2MASS 1632+1904 (Kirkpatrick et al. 1999), for both the SpeX and CGS4 datasets. These spectra effectively define the T dwarf class. The emergence of *H*-band CH_4 absorption at these spectral resolutions defines the start of the T dwarf sequence, as originally proposed by G02. Early-type T dwarfs exhibit weak CH_4 bands, strong H_2O bands and waning CO absorption at $2.3 \mu\text{m}$. In later types, H_2O and CH_4 bands progressively strengthen; the 1.05, 1.25, 1.6 and $2.1 \mu\text{m}$ peaks become more pronounced and acute; and the *K*-band peak becomes increasingly suppressed relative to *J*. The end of the T class is exemplified by the spectrum of 2MASS 0415–0935, with nearly saturated H_2O and CH_4 bands, and sharp triangular flux peaks emerging between these bands. The range of spectral morphologies encompassed by the standards in Figure 2 span the full spectral variety of the currently known T dwarf population.

3.2. Alternate Standards

In addition to the primary standards, we have identified a handful of alternate standards that have nearly identical near infrared spectral energy distributions but are well-separated on the sky. While in some cases these sources do not strictly adhere to the constraints outlined above, their purpose is to facilitate the observation of a spectral comparator at any time of the year. The alternate standards are listed in Table 2 and described as follows:

SDSS 0423–0414AB (T0 alternate): This relatively bright source ($J = 14.30 \pm 0.03$; Leggett et al. 2002b) was identified by G02. Its spectrum, like that of SDSS 1207+0244, exhibits exceedingly weak CH_4 absorption at *H*-band and both CO and CH_4 bands at *K*-band. SDSS 0423–0414AB was not selected as a primary standard here, however, as *HST* observations resolve it as an unequal-brightness binary (Burgasser et al. 2005). Nevertheless, its near infrared spectrum matches that of the T0 standard. SDSS 0423–0414AB has a parallax distance measurement of 15.2 ± 0.5 pc (Vrba et al. 2004).

SDSS 0151+1244 (T1 alternate): Identified by G02, this faint source ($J = 16.25 \pm 0.05$; Leggett et al. 2002b) is classified T1 on the G02 scheme. It is unresolved in *HST* images (Burgasser et al. in prep), and has a parallax distance measurement of 21.4 ± 1.6 pc (Vrba et al. 2004). Enoch,

Brown & Burgasser (2003) report significant K -band variability from this source (0.42 ± 0.14 mag peak-to-peak) with a possible period of 2.97 hours. The faintness and apparent variability of SDSS 0151+1244 relegate it as an alternate standard, although its near infrared spectrum is very similar to that of SDSS 0837–0000.

SDSS 1021–0304AB (T3 alternate): Identified by Leggett et al. (2000) and resolved as an unequal-brightness binary in *HST* observations (Burgasser et al. in prep), this original T3 standard on the B02 scheme (also classified T3 by G02) remains a viable alternative to the primary standard 2MASS 1209–1004, although it is only separated by 28° on the sky. SDSS 1021–0304AB has a parallax distance measurement of 29 ± 4 pc (Tinney, Burgasser, & Kirkpatrick 2003, see also Vrba et al. 2004).

2MASS 0755+2212 (T5 alternate): Identified by B02 and classified T5 on that system, this source has a nearly identical spectrum to that of the brighter T5 standard 2MASS 1503+2525 (Figure 3). It is unresolved in *HST* images (Burgasser et al. in prep). No parallax measurement has been reported.

2MASS 1553+1532AB (T7 alternate): This late-type T dwarf identified by B02 and classified T7 on that scheme has a near infrared spectrum identical to that of the T7 primary standard 2MASS 0727+1710. Resolved into an equal-magnitude, co-moving pair with *HST* and ground-based observations (Burgasser et al. in prep), 2MASS 1553+1532AB appears to be composed of two T dwarfs with similar spectral types. No parallax measurement has been reported for this source.

4. Methods of Classification

4.1. Direct Spectral Comparison

The most straightforward and accurate means of classifying any stellar spectrum is through the direct comparison of that spectrum to an equivalent set of spectral standards. Direct spectral comparison enables the simultaneous examination of multiple features, providing a broad match to the overall spectral morphology. Furthermore, this method facilitates the identification of peculiar sources which do not fit within the standard sequence, possibly due to secondary parameters or the presence of an unresolved companion (see § 6). Direct spectral comparison is the proscribed means of classification via the MK Process (Morgan & Keenan 1973).

Spectral types for all of the T dwarfs in the SpeX and CGS4 datasets were determined by overlaying their normalized spectra onto the corresponding T dwarf standard sequences⁵ shown in Figure 2. The standard sequences were augmented with near infrared data for the L8 optical

⁵With two exceptions: we used the alternate standard SDSS 0423–0414AB as the T0 comparator for the SpeX dataset, and SpeX cross-dispersed data were used for the T5 standard 2MASS 1503+2525 in the CGS4 dataset.

standard 2MASS 1632+1904 (Kirkpatrick et al. 1999); and for 2MASS 0310+1628 (Kirkpatrick et al. 2000), classified L9 in the near infrared by G02. Both source and standard spectra were normalized and compared in a consistent manner depending on the dataset. For the low resolution SpeX data, the entire 0.8–2.5 μm range was examined simultaneously after normalizing at the *J*-band flux peak. For the CGS4 data, spectra were separately normalized and compared in three wavebands — 0.95–1.35, 1.45–1.8 and 1.9–2.4 μm — to minimize errors in order scaling and to discern finer details. Examples of each of these methods is shown in Figures 3 and 4.

In both cases, subtypes for individual T dwarfs were assigned according to which standard spectra provided the closest spectral match. This was gauged by the relative strengths of the major H₂O and CH₄ bands, detailed shapes of the flux peaks and overall spectral slope. Half-subtypes were assigned for those spectra that clearly fell between standards (e.g., 2MASS 0559–1404 in Figure 4). While this comparative technique is qualitative in nature, the distinct spectral morphologies of the standard spectra enabled unambiguous classifications in nearly all cases. As the sequence is set up in whole subtype intervals, the nominal precision of the scheme is 0.5 subtypes for reasonable signal-to-noise (S/N) spectra. Classifications based on low S/N spectra are more uncertain and were specifically noted as such.

In some cases, the spectrum of a source does not fall anywhere in the standard sequence due to conflicting band strengths or substantially inconsistent broad band colors (the latter discernable with the SpeX prism data). These peculiar sources are exemplified in Figures 3 and 4 for the cases of 2MASS 0518–2828 (Cruz et al. 2004) and Gliese 229B (Nakajima et al. 1995; Geballe et al. 1996), respectively. Peculiar T dwarfs were specifically labelled and are discussed in further detail in § 6.

Tables 6 and 7 (column 9) list the resulting subtypes as determined by direct comparison for the SpeX and CGS4 sources, respectively. Subtypes for other data reported in the literature were also determined by comparing those spectra to standards obtained at similar resolution; e.g., Keck NIRC data were compared to the SpeX standards, while Keck NIRSPEC (low resolution) data were compared to the CGS4 standards. Derived spectral types for these data are given in Tables 8–12. In all cases, the classifications of sources with multiple spectral data are identical within the scheme’s 0.5 subclass precision. The consistency of the classifications demonstrates the reliability of the direct spectral comparison technique.

4.2. Classification by Spectral Indices

In cases where one is dealing with large spectral samples or desires a quantification of deviations from the standard system (e.g., when dealing with dust or gravity effects; see § 5.2), measurements of diagnostic features through spectral indices can be useful. Such indices, typically defined as the ratio of spectral flux or flux density in two different wavebands, have had widespread use in the classification of late-type dwarfs, whose spectra typically have strong molecular and atomic

features. For example, optical TiO and CaH indices defined by Reid, Hawley & Gizis (1995) and employed by Gizis (1997) are used to segregate solar metallicity and metal-poor M dwarfs; while near infrared indices have been widely employed in the classification of M and L dwarfs (Jones et al. 1994, 1996; Delfosse et al. 1997, 1999; Tinney et al. 1998; Tokunaga & Kobayashi 1999; Reid et al. 2001; Testi et al. 2001). Both B02 and G02 make use of spectral indices in their classifications, sampling the major H₂O and CH₄ bands, the 0.8–1.0 μm red slope, color ratios and the detailed shapes of the *J*- and *K*-band flux peaks. We revisit a subset of these indices here.

4.2.1. Revised Spectral Indices

The 1.1, 1.4 and 1.8 μm H₂O and 1.3, 1.6 and 2.2 μm CH₄ absorption bands are the most dominant and defining features of T dwarf spectra. These bands vary significantly and monotonically throughout the standard sequence and are generally correlated — strong H₂O bands are generally associated with strong CH₄ bands. These bands are also broad enough to be measured at low spectral resolutions, and are found in multiple spectral regions throughout the 1.0–2.5 μm range. Because of their utility, our spectral index analysis is focused on these strong molecular features.

We reexamined the H₂O and CH₄ indices defined in B02 and G02 in order to optimize their use with T dwarf spectra. They are redefined here as the ratio of the integrated flux over a spectral window within an absorption feature to the integrated flux over the same-sized window in the neighboring pseudocontinuum. This definition minimizes large fluctuations arising from poor S/N at the bottom of strong bands (e.g., in the latest-type T dwarfs). We also attempted to avoid regions of strong telluric absorption in order to minimize variations between spectra obtained at different sites. Finally, the spectral ratio wavebands were defined to be broad enough to facilitate use with both low and moderate spectral resolution data.

Table 3 lists the six revised classification indices, along with a seventh index measuring the ratio of flux between the *K*- and *J*-band flux peaks. This last index samples the relative strength of H₂ absorption, a gravity and metallicity-sensitive feature (e.g., B02), and is discussed in further detail in § 5.2. Figure 5 diagrams the passbands of the H₂O and CH₄ indices on the spectrum of the T5 standard 2MASS 1503+2525 and a telluric absorption spectrum typical of Mauna Kea.⁶

Measurements of the redefined indices for spectral data examined here are given in Tables 6–12 (columns 2–8). In Figures 6 and 7, we plot the values of the H₂O and CH₄ indices as measured with the SpeX and CGS4 data, respectively, as a function of spectral type. All six ratios show monotonic decreases in value with later subtypes, with strong correlations. In particular, the H₂O-H index varies nearly linearly over the entire spectral type range. The H₂O-J, CH₄-J and CH₄-H indices are slightly degenerate for the earliest T spectral types, while the CH₄-K index is degenerate between T7 and T8. The index H₂O-K shows the largest scatter as a function of spectral type, notably

⁶These data, produced using the program IRTRANS4, were obtained from the UKIRT worldwide web pages.

among late-type and peculiar sources. Indeed, for some datasets (e.g., OSIRIS), there is very poor correlation between this index and spectral type, likely due to increased noise caused by telluric absorption around the 1.9 μm H₂O band. We therefore omit this index from our classification set, and focus on five primary classification indices: H₂O-J, CH₄-J, H₂O-H, CH₄-H and CH₄-K.

4.2.2. Index Classification: Two Methods

The B02 and G02 schemes differ slightly in their use of spectral indices for classification. The former scheme directly compares measured indices to those of the standards, while the latter scheme specifies subtype ranges for each index. The B02 method is more closely aligned to the MK Process in spirit, but the G02 method is a less cumbersome means of determining the classification of a particular T dwarf. As both of these techniques have been used in the literature, we examined them independently to determine whether any significant differences exist.

Index subtypes were first derived following the prescription of B02. Table 4 lists the spectral index values for the T dwarf standards with SpeX and CGS4 data, in addition to values for the L8 and L9 comparison stars 2MASS 1632+1904 and 2MASS 0310+1648. As in B02, individual index subtypes were first determined as the closest match to the standard values (or half-subtype match). Subtypes for the CH₄-H index were only used for index values less than 1.0, as higher values are degenerate for L dwarfs and the earliest T dwarfs. Final classifications were determined as the average of the index subtypes; no rejection of outliers was made as in B02. Sources with a large scatter amongst the index subtypes (> 1 subclass) or with only one spectral index measure available were noted as uncertain.

The second method, following the prescription of G02, involves the comparison of spectral indices to predefined ranges. Table 5 lists these ranges for the new indices, determined as the typical values for each spectral type as measured on the CGS4 data (i.e., Figure 7). Because of their degeneracy, ranges for the H₂O-J and CH₄-K indices are only defined for spectral types \geq T2 and \leq T6, respectively. Index subtypes for each T dwarf were assigned according to the range the value falls in (or half subtype for values close to range borders), and the average type was determined in the manner described above.

Tables 6–12 list the index-based spectral subtypes for the five primary classification ratios (columns 2-6) as well as the averaged types for all indices (columns 10-11). These classifications are generally equivalent to those determined by direct spectral comparison, as demonstrated in Figures 8 and 9 for the SpeX dataset. Differences between the direct comparison and index-based classifications are generally less than 0.5-1 subtypes, with typical deviations of 0.3 subtypes. Hence, all three techniques yield results that are consistent within the nominal 0.5 subtype uncertainty of the scheme, and any could be used to classify the spectrum of a T dwarf. It is important to stress, however, that spectral indices are only proxies for the overall spectral morphology of a source, and direct spectral comparison to the standards is the most accurate and consistent means

of classification (Morgan & Keenan 1973).

5. Discussion

5.1. Revised Spectral Types and T Dwarf Properties

The revised classification scheme for T dwarfs presented here is similar in design to the schemes proposed by B02 and G02, both in the choice of spectral standards and spectral indices. Table 13 confirms this, comparing revised spectral types for 61 T dwarfs (based on direct spectral comparison) to prior classifications made on the B02 and G02 schemes. Nearly all of these are consistent within 0.5 subtypes; only seven differ by a full subclass (including the peculiar T7 Gliese 229B; see below). Hence, previously identified trends of absolute brightness (Dahn et al. 2002; Tinney, Burgasser, & Kirkpatrick 2003; Vrba et al. 2004), color (Burgasser et al. 2002c; Leggett et al. 2002b; Knapp et al. 2004) and T_{eff} (Golimowski et al. 2004; Vrba et al. 2004) as a function of spectral type remain effectively unchanged.

Studies to date have demonstrated that for subtypes T5 and later, T spectral types are largely correlated with T_{eff} and luminosity (Golimowski et al. 2004; Vrba et al. 2004). This result is broadly consistent with the observed correlation between MK numerical type and temperature for main sequence stars. However, the temperature correlation for earlier-type T dwarfs is weak, with T_{eff} roughly constant from L8 to T5 despite significant changes in near infrared spectral energy distributions (Kirkpatrick et al. 2000; Burgasser et al. 2002c; Dahn et al. 2002; Tinney, Burgasser, & Kirkpatrick 2003; Golimowski et al. 2004; Nakajima et al. 2004; Vrba et al. 2004). The unusual properties of this spectral morphological transition, as well as the significant color variations found among similarly-typed late-type T dwarfs (Knapp et al. 2004; Burgasser, Burrows & Kirkpatrick 2005), suggest that further extensions to the one dimensional scheme defined here may be required. However, the clear variation in spectral morphologies of the standard stars across this transition imply that the scheme itself need not be redefined.

5.2. Extending the T Dwarf Spectral Sequence

5.2.1. Dust Effects in Early-type T Dwarf Spectra

Condensate dust strongly influences the near infrared spectra of L dwarfs and early-type T dwarfs, but is largely absent in late-type T dwarf atmospheres (Tsuji et al. 1996; Allard et al. 2001). The depletion of dust from cool brown dwarf photospheres is now believed to play a greater role in the spectral transition between L and T dwarfs than T_{eff} (Ackerman & Marley 2001; Burgasser et al. 2002c; Tsuji & Nakajima 2003), although the mechanism for this depletion remains under considerable debate (Burgasser et al. 2002b; Knapp et al. 2004; Tsuji 2005). The composition and abundance of condensate dust species, and the thickness, density and surface distribution

of condensate cloud structures (Ackerman & Marley 2001), are likely to be complex functions of T_{eff} , surface gravity, metallicity, rotation and other parameters (Helling et al. 2001, 2004; Lodders 2002; Woitke & Helling 2003, 2004); hence, substantial spectral variations among dust-dominated sources might be expected. Indeed, there appears to be a decoupling of optical and near infrared spectral morphologies among late-type L dwarfs and early-type T dwarfs that could be indicative of such dust/ T_{eff} effects (Cruz et al. 2003; Knapp et al. 2004). A few of the early-type T dwarfs (e.g., 2MASS 0949–1545 and 2MASS 2139+0220; Tinney et al. 2005; Cruz et al. in prep.), while having overall spectral morphologies consistent with T1–T2 dwarfs, exhibit a much broader range of band strengths (and hence larger scatter in their index subtypes) and $J - K_s$ colors. While unresolved multiplicity cannot be ruled out for these sources (§ 6), the possible influence of dust-related spectral variations falls beyond the one-dimensional scheme defined here, and may require an additional classification parameter.

The temporal evolution of dust-sensitive spectral features must also be characterized, particularly as this directly affects the stability of the spectral standards. While a number of studies have measured photometric variability of up to 0.5 mag in several L and T dwarfs (Bailer-Jones & Mundt 1999, 2001; Tinney & Tolley 1999; Gelino et al. 2002; Enoch, Brown & Burgasser 2003; Bailer-Jones & Lamm 2003; Koen 2003, 2004), only one T dwarf has been monitored for spectral variations so far (SDSS 1624+0029; Nakajima et al. 2000). As the photometric variations have been linked to the surface evolution of condensate dust clouds (Gelino et al. 2002; Mohanty et al. 2002), verifying the spectral stability of the earliest-type T standards, which are most affected by the photospheric condensates, should be a priority for future observational studies.

5.2.2. Gravity Effects in Late-type T Dwarf Spectra

On the other end of the sequence, a handful of late-type T dwarfs, which exhibit otherwise normal band strengths, show significant variations in their K -band flux peaks as compared to the spectral standards. This phenomenon, cited extensively in the literature (Burgasser et al. 2002c, 2004a; Burgasser, Burrows & Kirkpatrick 2005; Leggett et al. 2002b; Golimowski et al. 2004; Knapp et al. 2004), is caused by variations in collision induced H_2 absorption, which is particularly strong in the atmospheres of the coldest brown dwarfs. Correlated variations are also seen in the strengths of the $1.25 \mu\text{m}$ K I lines (Knapp et al. 2004) and the $1.05 \mu\text{m}$ flux peak (Burgasser, Burrows & Kirkpatrick 2005). These spectral peculiarities are likely tied to differences in surface gravities and possibly metallicities among late-type T dwarfs (Saumon et al. 1994; Burrows et al. 2002a; Burgasser, Burrows & Kirkpatrick 2005; Knapp et al. 2004), and can vary significantly for a given set of H_2O and CH_4 band strengths. This is demonstrated graphically in Figure 10, which compares the K/J and CH_4-H ratios for the SpeX prism dataset.⁷ While the ratios show reasonable correlation

⁷The SpeX dataset is particularly useful for exploring this phenomenon as the entire $0.8\text{--}2.5 \mu\text{m}$ range is observed in a single dispersion order, mitigating flux scaling errors that can affect data obtained in multiple settings.

over much of the T sequence, there is a substantial increase in the range of K/J values amongst the latest-type T dwarfs. The decoupling of these “surface gravity features” from the standard classification sequence again suggests that a second classification parameter is required to fully describe the spectra.

While dust, gravity and metallicity features may necessitate extensions to the one dimensional scheme defined here, the inclusion of a second (or third or fourth) classification parameter under the MK Process requires the identification of additional spectral standards to map out the new parameter space. As the number of “deviant” T dwarfs is still relatively small, we leave this task to a future study.

5.3. To the End of the T Dwarf Class and Beyond

The classification scheme defined here sufficiently encompasses the range of spectral morphologies observed for the known population of T dwarfs. But what about colder brown dwarfs that are likely to be identified in the near future? Assigning new T subtypes for such sources would require that they follow the same spectral trends as the latest-type T dwarfs, namely progressively stronger bands of H₂O and CH₄. As these bands are already nearly saturated in the spectrum of the T8 standard 2MASS 0415–0935, it is unlikely that many more *readily distinguishable* T subtypes will be identified (Burrows, Sudarsky & Lunine 2003). This is not to say that significantly cooler brown dwarfs could not be classified as late-type T dwarfs; these later subtypes may just encompass much broader T_{eff} intervals. Furthermore, there is no *a priori* reason that T subtypes could not extend to T10 and beyond, as is the case for the M giant sequence.

On the other hand, if the near infrared spectral features of a cold brown dwarf discovery were significantly and systematically different than those examined here, a new spectral class, already referred to in the literature as the Y dwarf class (Kirkpatrick et al. 1999; Burrows, Sudarsky & Lunine 2003; Knapp et al. 2004), would be required. How will these spectra differ? Theoretical atmosphere models predict several effects, including the emergence of NH₃ bands at 1.5 and 1.95 μm below $T_{eff} \sim 600$ K (the 10.5 μm band has already been detected in the spectrum of Epsilon Indi Bab; Roellig et al. 2004); the disappearance of the strong pressure-broadened Na I and K I doublets, and weaker Cs I lines at 0.85 and 0.89 μm , below $T_{eff} \sim 500$ K; the condensation of H₂O vapor around 400–500 K; and the gradual transition to red near infrared spectral energy distributions around 300–400 K (Burrows, Sudarsky & Lunine 2003). Any of these near infrared spectral transitions would signal a clear break between the T and Y spectral classes. Such a break could also arise at other wavelengths. Just as T dwarfs are distinguished from the (originally) optically-classified L dwarfs by the presence of the near infrared CH₄ bands (Kirkpatrick et al. 1999; Geballe et al. 2002), so too may Y dwarfs be distinguished by the emergence of distinct features longward of 2.5 μm , such as the 2.95 μm NH₃ band or broad H₂ features beyond 10 μm (Burrows, Sudarsky & Lunine 2003). Until examples of these cold brown dwarfs are actually identified, however, delineating the end of the T dwarf class is largely an exercise in speculation.

6. Individual Sources

A handful of sources studied here deserve additional attention, either due to their spectral peculiarity or significantly revised classification.

DENIS 0255–4700 (L9): Identified by Martín et al. (1999) in the Deep Near Infrared Survey of the Southern Sky (DENIS; Epchtein et al. 1997), this relatively bright L dwarf (2MASS $J=13.25\pm0.03$) is classified L8 in the optical (Kirkpatrick et al. in prep.). Cushing, Rayner & Vacca (2005) have detected weak CH₄ absorption at 1.6 and 2.2 μm in moderate resolution SpeX data, and suggest that this source could be classified as a T dwarf based on the definition put forth by G02. However, it is important to note that the analogous definition adopted here requires the detection of *H*-band CH₄ absorption at low spectral resolutions. Examination of SpeX prism data (Burgasser et al. in prep.; Figure 11) reveals no distinct *H*-band CH₄ absorption feature (likely due to its weakness) and an overall spectral energy distribution consistent with a late-type L dwarf. Therefore, according to the scheme defined here, DENIS 0255–4700 is classified $\sim\text{L9}$ in the near infrared, of slightly earlier type than a T dwarf.

SDSS 1104+5548 and SDSS 2047–0718 (T0): Classified $\text{L9.5}\pm1.5$ and $\text{L9.5}\pm1.0$ by G02, respectively, these faint sources are reclassified T0: based on their similarity to the T0 standard SDSS 1207+0244. Weak CH₄ absorption appears to be present at both 1.6 and 2.2 μm , although the low S/N spectra of both sources make these assignments uncertain.

2MASS 0518–2828 (T1p): The spectrum of this source is clearly peculiar (Figure 3), with *J*- and *H*-band spectral features consistent with a subtype later than T2, but a *K*-band spectrum and red *J* – *K* color consistent with a late-type L dwarf/early-type T dwarf. Cruz et al. (2004), who identified the source in the 2MASS database, have proposed that it is an unresolved binary composed of a mid/late-type L dwarf ($\sim\text{L6}$) and early/mid-type T dwarf ($\sim\text{T4}$). Confirmation of this hypothesis is forthcoming (Cruz 2005, priv. comm.).

2MASS 0920+3517AB (T0p): This source was identified by Kirkpatrick et al. (2000) in the 2MASS database and is classified L6.5 in the optical. Spectroscopic observations by Nakajima et al. (2001) reveal the presence of CH₄ absorption at 1.6 and 2.2 μm , which are verified, but previously unrecognized, in low resolution NIRC grism data (B02; Figure 11). However, there are some spectral discrepancies; the 1.1 μm H₂O/CH₄ band is shallower than those observed in early-type T dwarfs, while the 2.2 μm CH₄ band is fairly weak compared to the 1.6 μm band. Like 2MASS 0518–2828, these features may arise from a composite spectrum of a late-type L dwarf and early-type T dwarf pair. 2MASS 0920+3517AB is marginally resolved as a closely-separated ($\sim0''.075$) binary in *HST* observations (Reid et al. 2001).⁸ Bouy et al. (2003) determine an F814W ($\lambda_c = 0.83 \mu\text{m}$) flux ratio of 0.88 ± 0.11 mag, implying $M_I \approx 19$ for 2MASS 0920+3517B, comparable to the *I*-band absolute magnitudes of late-type L dwarfs through mid-type T dwarfs (Dahn et al. 2002). A composite

⁸Reid et al. (2001) also speculate that the 2MASS 0850–1057AB system, the L6 spectral standard on the Kirkpatrick et al. (1999) optical scheme, may harbor a T dwarf secondary.

L/T spectrum might also explain the large discrepancy between the optical spectral type and near infrared spectral morphology of this source.

Gliese 337CD (T0): Identified by Wilson et al. (2001b) as a widely separated ($43'' \approx 880$ AU) common proper motion companion to the G8V+K1V binary Gliese 337AB, and itself resolved as a nearly equal brightness binary at *K*-band (Burgasser, Kirkpatrick & Lowrance 2005), this source is optically classified L8 on the Kirkpatrick et al. (1999) scheme. Its near infrared spectrum (McLean et al. 2003) exhibits distinct signatures of CH₄ absorption at both 1.6 and 2.2 μm that are similar to features in the T0 standard SDSS 1207+0244. The composite spectrum is therefore reclassified T0 here. The small difference in absolute *K*-band magnitudes from L8–T4 (Tinney, Burgasser, & Kirkpatrick 2003; Golimowski et al. 2004; Vrba et al. 2004) suggests that this system could also be composed of a late-type L dwarf and early-type T dwarf pair.

2MASS 0937+2931 (T6p): The prototype example of photospheric pressure effects in T dwarf spectra (§ 5.2.2), this peculiar T6 has been discussed extensively in the literature (Burgasser et al. 2002c, 2003b; Golimowski et al. 2004; Knapp et al. 2004; Vrba et al. 2004; Burgasser, Burrows & Kirkpatrick 2005). The current scheme retains the T6 classification of B02, but spectral peculiarities are clearly evident in both low resolution (enhanced 1.05 μm peak, suppressed *K*-band peak) and moderate resolution (weak 1.25 μm K I lines) data. 2MASS 0034+0523, 2MASS 0939–2448 and 2MASS 1114–2618 show similar, albeit less pronounced, spectral deviations (Burgasser et al. 2004a; Burgasser, Burrows & Kirkpatrick 2005); while SDSS 1110+0116 exhibits enhanced *K*-band flux, suggesting that it is a low gravity source (Knapp et al. 2004). The peculiar status of 2MASS 0937+2931 may therefore simply reflect the shortcomings of the one-dimensional classification scheme defined here.

Gliese 229B (T7p): One of the first brown dwarfs to be identified (Nakajima et al. 1995; Oppenheimer et al. 1995), this prototype T dwarf nevertheless fails to fit cleanly within the sequence of spectral standards. As shown in Figure 4, the CGS4 spectrum of Gliese 229B (Geballe et al. 1996) exhibits strong CH₄ absorption at 1.3 and 1.6 μm consistent with a T7 spectral type; but weaker H₂O and CH₄ bands at 1.1, 1.4, 1.9 and 2.2 μm , consistent with type T5–T6. Low resolution NIRC grism data (Oppenheimer et al. 1998) show similar deviations. Because of its early discovery, there have been several detailed studies of Gliese 229B suggesting that it may have atypical physical properties. Griffith, Yelle & Marley (1998) and Griffith & Yelle (2000) have proposed that the metallicity of Gliese 229B may be 0.3–0.5 solar, based on spectral model fits to H₂O and Cs I features in its optical spectrum. Using spectral model fits for the M1V primary, Leggett et al. (2002a) have also concluded that this system is metal-poor and possibly young as well. Both Gliese 229B and 2MASS 0937+2931 are therefore important sources for studying the role of surface gravity and metallicity on the emergent spectra of the coldest known brown dwarfs.

7. Summary

We have defined a revised near infrared classification scheme for T dwarfs that unifies and supersedes original schemes proposed by B02 and G02. Nine primary spectral standards and five alternate standards define the scheme, and classifications for other sources may be made by the direct comparison of equivalent spectral data. Two alternate methods of classification using spectral indices have been described and shown to have no significant differences with direct spectral comparison. The revised classifications are also consistent with the prior schemes, implying that existing analyses of spectral type trends remain intact. Nonetheless, we point out that future extensions to the one dimensional classification scheme presented here may be needed to incorporate additional spectral variations. These extensions may be made when more examples of these objects are identified and characterized.

In the Appendix, we provide a compendium of all T dwarfs with published near infrared spectra at the time this article was written, listing classifications on the revised scheme. With 69 systems comprising this census, the study of cold brown dwarfs has crossed a threshold where detailed comparative analyses, population statistics and the discovery and characterization of physically unique sources can be made. As forthcoming deep and wide-field sky surveys (e.g., UKIDSS, Warren 2002) uncover many more of our T dwarf neighbors, a unified framework for classifying these objects is clearly essential.

The authors give special thanks to K. Cruz, J. G. Cuby, M. Cushing, M. Liu, M. McCaughrean, I. S. McLean, T. Nakajima, B. Oppenheimer, R.-D. Scholz and M. R. Zapatero Osorio for providing published and unpublished spectral data for this work, and to K. Chiu and X. Fan for assistance with the retrieval of SDSS photometry. A. J. B. also thanks C. Corbally and R. Gray for useful insights on the MK Process. We thank our anonymous referee for her/his helpful critique of the original manuscript. A. J. B. acknowledges support from NASA through the SIRTf Fellowship Program. T. R. G. acknowledges support by the Gemini Observatory, which is operated by the Association of Universities for Research in Astronomy, Inc., on behalf of the international Gemini partnership of Argentina, Australia, Brazil, Canada, Chile, the United Kingdom and the United States of America. Some data were obtained through the UKIRT Service Programme. UKIRT is operated by the Joint Astronomy Centre on behalf of the UK Particle Physics and Astronomy Research Council. This publication makes use of data from the Two Micron All Sky Survey, which is a joint project of the University of Massachusetts and the Infrared Processing and Analysis Center, and funded by the National Aeronautics and Space Administration and the National Science Foundation. 2MASS data were obtained from the NASA/IPAC Infrared Science Archive, which is operated by the Jet Propulsion Laboratory, California Institute of Technology, under contract with the National Aeronautics and Space Administration. Funding for the Sloan Digital Sky Survey (SDSS) has been provided by the Alfred P. Sloan Foundation, the Participating Institutions, the National Aeronautics and Space Administration, the National Science Foundation, the U.S. Department of Energy, the Japanese Monbukagakusho, and the Max Planck Society. The SDSS

Web site is <http://www.sdss.org/>. The SDSS is managed by the Astrophysical Research Consortium (ARC) for the Participating Institutions. The Participating Institutions are The University of Chicago, Fermilab, the Institute for Advanced Study, the Japan Participation Group, The Johns Hopkins University, the Korean Scientist Group, Los Alamos National Laboratory, the Max-Planck-Institute for Astronomy (MPIA), the Max-Planck-Institute for Astrophysics (MPA), New Mexico State University, University of Pittsburgh, University of Portsmouth, Princeton University, the United States Naval Observatory, and the University of Washington.

A. T Dwarf Compendium

Table 14 provides a compendium of all T dwarfs with published near infrared spectra at the writing of this article, and a sample of their empirical properties. This list includes 69 systems, including nine binaries and four companions to main sequence stars. Near infrared spectral types on the revised scheme are provided in column 2. Equinox J2000 coordinates, listed in columns 3 and 4, are primarily from the 2MASS All Sky Point Source Catalog (Cutri et al. 2003) with the exceptions of IFA 0226+0051, S Ori 70, SDSS 0837–0000, SDSS 1104+5548, SDSS 1157+0611, NTTDF 1205–0744, SDSS 1632+4150 and SDSS 2047-0718 for which positional data were obtained from the SDSS catalog or the discovery reference. Coordinate epochs are given in column 5. SDSS z -band magnitudes on the AB asinh system (Fukugita et al. 1996; Lupton, Gunn & Szalay 1999) from the SDSS Data Release 4 (Adelman-McCarthy et al. 2005) are listed in column 6. 2MASS JHK_s photometry from the All Sky Catalog is listed in columns 7–9; for those sources undetected or marginally detected by 2MASS, alternate CIT or MKO⁹ JHK photometry is provided. Parallax (π ; column 10) and proper motion (μ , ϕ ; columns 11 and 12) measurements from Dahn et al. (2002); Tinney, Burgasser, & Kirkpatrick (2003); and Vrba et al. (2004) are listed for field sources; and from HIPPARCOS (ESA 1997) for T dwarf companions to main sequence stars. Additional proper motion measurements from Burgasser et al. (2003c, 2004a); Burgasser, McElwain, & Kirkpatrick (2003); Ellis et al. (2005); and Tinney et al. (2005) are also listed. Relevant publications, including discovery citations, are provided in column 13. An electronic version of this table will be made available through the journal.

REFERENCES

- Ackerman, A. S., & Marley, M. S. 2001, *ApJ*, 556, 872
- Adelman-McCarthy, J., et al. 2005, *ApJS*, submitted

⁹Note that photometry on the MKO system can be very different from photometry on the 2MASS or CIT systems. Values measured for T dwarfs in the former system can be found in Leggett et al. (2002b) and Knapp et al. (2004), and transformations between the MKO and 2MASS systems for late-type dwarfs are given in Stephens & Leggett (2004).

- Allard, F., Hauschildt, P. H., Alexander, D. R., Tamanai, A., & Schweitzer, A. 2001, *ApJ*, 556, 357
- Bailer-Jones, C. A. L., Coryn A. L., Irwin, M., & von Hippel, T. 1998, *MNRAS*, 298, 361
- Bailer-Jones, C. A. L., & Lamm, M. 2003, *MNRAS*, 339, 477
- Bailer-Jones, C. A. L., & Mundt, R. 1999, *A&A*, 348, 800
- . 2001, *A&A*, 367, 218
- Borysow, A., Jørgensen, U. G., & Zheng, C. 1997, *A&A*, 324, 185
- Bouy, H., Brandner, W., Martín, E. L., Delfosse, X., Allard, F., & Basri, G. 2003, *AJ*, 126, 1526
- Burgasser, A. J., Burrows, A., & Kirkpatrick, J. D. 2005, *ApJ*, submitted
- Burgasser, A. J., Geballe, T. R., Golimowski, D. A., Leggett, S. K., Kirkpatrick, J. D., Knapp, G. R., & Fan, X. 2003a, in *Brown Dwarfs: Proceedings of IAU Symposium 211*, ed. E. Martín (San Francisco: ASP), p. 377
- Burgasser, A. J., Liebert, J., Kirkpatrick, J. D., & Gizis, J. E. 2002a, *AJ*, 123, 2744
- Burgasser, A. J., Kirkpatrick, J. D., Liebert, J., & Burrows, A. 2003b, *ApJ*, 594, 510
- Burgasser, A. J., Kirkpatrick, J. D., & Lowrance, P. J. 2005, *AJ*, 129, 2849
- Burgasser, A. J., Kirkpatrick, J. D., McElwain, M. W., Cutri, R. M., Burgasser, A. J., & Skrutskie, M. F. 2003c, *AJ*, 125, 850
- Burgasser, A. J., Kirkpatrick, J. D., Reid, I. N., Brown, M. E., Miskay, C. L., & Gizis, J. E. 2003d, *ApJ*, 586, 512
- Burgasser, A. J., Kirkpatrick, J. D., Reid, I. N., Liebert, J., Gizis, J. E., & Brown, M. E. 2000a, *AJ*, 120, 473
- Burgasser, A. J., Marley, M. S., Ackerman, A. S., Saumon, D., Lodders, K., Dahn, C. C., Harris, H. C., & Kirkpatrick, J. D. 2002b, *ApJ*, 571, L151
- Burgasser, A. J., McElwain, M. W., & Kirkpatrick, J. D. 2003, *AJ*, 126, 2487
- Burgasser, A. J., McElwain, M. W., Kirkpatrick, J. D., Cruz, K. L., Tinney, C. G., & Reid, I. N. 2004a, *AJ*, 127, 2856
- Burgasser, A. J., Reid, I. N., Kirkpatrick, J. D., Leggett, S. K., Liebert, J., & Burrows, A. 2005, *ApJ*, submitted
- Burgasser, A. J., et al. 1999, *ApJ*, 522, L65
- . 2000b, *ApJ*, 531, L57

- . 2000c, *AJ*, 120, 1100
- . 2002c, *ApJ*, 564, 421 (B02)
- Burrows, A., Burgasser, A. J., Kirkpatrick, J. D., Liebert, J., Milsom, J. A., Sudarsky, D., & Hubeny, I. 2002a, *ApJ*, 573, 394
- Burrows, A., Hubbard, W. B., Lunine, J. I., & Liebert, J. 2001, *Rev. of Modern Physics*, 73, 719
- Burrows, A., Sudarsky, D., & Lunine, J. I. 2003, *ApJ*, 596, 587
- Cannon, A. J., & Pickering, E. C. 1918-1924, *Ann. Astron. Obs. Harvard College*, 91-99
- Corbally, C. J., Gray R. O., & Garrison, R. F. 1994, *The MK process at 50 years. A Powerful Tool for Astrophysical Insight* (San Francisco: Astronomical Society of the Pacific)
- Cruz, K. L., Reid, I. N., Liebert, J., Kirkpatrick, J. D., & Lowrance, P. J. 2003, *AJ*, 126, 2421
- Cruz, K. L., Burgasser, A. J., Reid, I. N., & Liebert, J., 2004, *ApJ*, 604, L61
- Cuby, J. G., Saracco, P., Moorwood, A. F. M., D’Odorico, S., Lidman, C., Comerón, F., & Spyromilio, J. 1999, *A&A*, 349, L41
- Cushing, M. C., Rayner, J. T., & Vacca, W. D. 2005, *ApJ*, 623, 1115
- Cushing, M. C., Vacca, W. D., & Rayner, J. T. 2004, *PASP*, 116, 362
- Cutri, R. M., et al. 2003, *Explanatory Supplement to the 2MASS All Sky Data Release*, <http://www.ipac.caltech.edu/2mass/releases/allsky/doc/explsup.html>
- Dahn, C. C., et al. 2002, *AJ*, 124, 1170
- Delfosse, X., et al. 1997, *A&A*, 327, L25
- . 1999, *A&A*, 351, L5
- Depoy, D. L., Atwood, B., Byard, P. L., Frogel, J., & O’Brien, T. P. 1993, in *Proceedings of SPIE*, Vol. 1946, ed. A. M. Fowler (Bellingham: SPIE), 667
- Ellis, S. C., Tinney, C. G., Burgasser, A. J., Kirkpatrick, J. D., & McElwain, M. W. 2005, *AJ*, in press
- Epchtein, N., et al. 1997, *The Messenger*, 87, 27
- Enoch, M. L., Brown, M. E., & Burgasser, A. J. 2003, *AJ*, 126, 1006
- ESA, 1997, *The Hipparcos and Tycho Catalogues*, ESA SP-1200
- Fukugita, M., Ichikawa, T., Gunn, J. E., Doi, M., Shimasaku, K., & Schneider, D. P. 1997, *AJ*, 111, 1748

- Garrison, R. F. 1984, *The MK Process and Stellar Classification: Proceedings of the Workshop in Honour of W. W. Morgan and P. C. Keenan* (Toronto: David Dunlap Observatory)
- Geballe, T. R., Kulkarni, S. R., Woodward, C. E., & Sloan, G. C. 1996, *ApJ*, 467, 101
- Geballe, T. R., Saumon, D., Leggett, S. K., Knapp, G. R., Marley, M. S., & Lodders, K. 2001, *ApJ*, 556, 373
- Geballe, T. R., et al. 2002, *ApJ*, 564, 466 (G02)
- Gelino, C. R., Marley, M. S., Holtzman, J. A., Ackerman, A. S., & Lodders, K. 2002, *ApJ*, 577, 433
- Golimowski, D. A., Burrows, C. S., Kulkarni, S. R., Oppenheimer, B. R., & Brukardt, R. A. 1998, *AJ*, 115, 2579
- Golimowski, D. A., et al. 2004, *AJ*, 127, 3516
- Gizis, J. E. 1997, *AJ*, 113, 806
- Griffith, C. A., & Yelle, R. V. 2000, *ApJ*, 532, L59
- Griffith, C. A., Yelle, R. V., & Marley, M. S. 1998, *Science*, 282, 2063
- Hayashi, C., & Nakano, T. 1963, *Prog. Theo. Physics*, 30, 4
- Helling, C., Klein, R., Woitke, P., Nowak, U., & Sedlmayr, E. 2004, *A&A*, 423, 657
- Helling, C., Oevermann, M., Lüttke, M. J. H., Klein, R., & Sedlmayr, E. 2001, *A&A*, 376, 194
- von Hippel, T., Storrie-Lombardi, L. J., Storrie-Lombardi, M. C., & Irwin, M. J. 1994, *MNRAS*, 269, 97
- Houk, N. 1978, *Michigan Catalogue of Two-Dimensional Spectral Types for the HD Stars. Vol. 2: Declinations -53 to -40 degrees* (Ann Arbor: Univ. Michigan)
- Houk, N. 1982, *Michigan Catalogue of Two-Dimensional Spectral Types for the HD Stars. Vol. 3: Declinations -40 to -26 degrees* (Ann Arbor: Univ. Michigan)
- Houk, N., & Cowley, A. P. 1978, *Michigan Catalogue of Two-Dimensional Spectral Types for the HD Stars. Vol. 1: Declinations -90 to -53 degrees* (Ann Arbor: Univ. Michigan)
- Houk, N., & Smith-Moore, M. 1988, *Michigan Catalogue of Two-Dimensional Spectral Types for the HD Stars. Vol. 4: -26 to -12 degrees* (Ann Arbor: Univ. Michigan)
- Houk, N., & Swift, C. 1999, *Michigan Catalogue of Two-Dimensional Spectral Types for the HD Stars. Vol. 5* (Ann Arbor: Univ. Michigan)
- Hubble, E. 1936, *The Realm of the Nebulae* (New Haven: Yale University Press)

- Jones, H. R. A., Longmore, A. J., Allard, F., & Hauschildt, P. H. 1996, *MNRAS*, 280, 77
- Jones, H. R. A., Longmore, A. J., Jameson, R. F., & Mountain, C. M. 1994, *MNRAS*, 267, 413
- Keenan, P. C., & McNeil, R. C. 1976, *An Atlas of Spectra of the Cooler Stars: Types G, K, M, S and C* (Columbus: Ohio State Univ. Press)
- Kirkpatrick, J. D., Henry, T. J., & McCarthy, D. W., Jr. 1991, *ApJS*, 77, 417
- Kirkpatrick, J. D., Reid, I. N., Liebert, J., Gizis, J. E., Burgasser, A. J., Monet, D. G., Dahn, C. C., Nelson, B., & Williams, R. J. 2000, *AJ*, 120, 447
- Kirkpatrick, J. D., et al. 1999, *ApJ*, 519, 802
- Kobayashi, N., et al. 2000, *Proc. SPIE*, 4008, 1056
- Koen, C. 2004, */mnras*, 346, 473
- . 2004, */mnras*, 354, 378
- Kumar, S. S. 1962, *AJ*, 67, 579
- Knapp, G., et al. 2004, *ApJ*, 127, 3553
- Leggett, S. K., Hauschildt, P. H., Allard, F., Geballe, T. R., & Baron, E. 2002a, *MNRAS*, 332, 78
- Leggett, S. K., Toomey, D. W., Geballe, T. R., & Brown, R. H. 1999, *ApJ*, 517, L139
- Leggett, S. K., et al. 2000, *ApJ*, 536, L35
- . 2002b, *ApJ*, 564, 452
- Lenzen, R., et al. 1998, *Proc. SPIE*, 3354, 606
- Linnaeus, C. 1735, *Systema Naturae*
- Liu, M. C., Wainscoat, R., Martín, E. L., Barris, B., & Tonry, J. 2002, *ApJ*, 568, L107
- Lodders, K. 2002, *ApJ*, 577, 974
- Lupton, R. H., Gunn, J. E., & Szalay, A. S. 1999, *AJ*, 118, 1406
- Martín, E. L., Delfosse, X., Basri, G., Goldman, B., Forveille, T., & Zapatero Osorio, M. R. 1999, *AJ*, 118, 2466
- Martín, E. L., & Zapatero Osorio, M. R. 2003, *ApJ*, 593, L113
- Matthews, K., & Soifer, B. T. 1994, in *Infrared Astronomy with Arrays: The Next Generation*, ed. I. McLean (Dordrecht: Kluwer), 239

- McCaughrean, M., Close, L. M., Scholz, R.-D., Lenzen, R., Biller, B., Brandner, W., Hartung, M., & Lodieu, N. 2004, *A&A*, 413, 1029
- McLean, I. S., Graham, J. R., Becklin, E. E., Figer, D. F., Larkin, J. E., Levenson, N. A., & Teplitz, H. I. 2000, *SPIE*, 4008, 1048
- McLean, I. S., McGovern, M. R., Burgasser, A. J., Kirkpatrick, J. D., Prato, L., & Kim, S. 2003, *ApJ*, 596, 561
- McLean, I. S., et al. 1998, *SPIE*, 3354, 566
- Mendeleeff (Mendeleev), D. 1869, *Zeitschrift für Chemie*, 12, 405
- Mohanty, S., Basri, G., Shu, F., Allard, F., & Chabrier, G. 2002, *ApJ*, 572, 469
- Moorwood, A. F. 1997, *Proc. SPIE*, 2871, 1146
- Moorwood, A. F., Cuby, J.-G., & Lidman, C. 1998, *The Messenger*, 91, 9
- Morgan, W. W., Abt, H. A., & Tapscott, J. W. 1978, *Revised MK Spectral Atlas for Stars Earlier than the Sun (Williams Bay: Yerkes Observatory and Tucson: Kitt Peak National Observatory)*
- Morgan, W. W., & Keenan, P. C. 1973, *ARA&A*, 11, 29
- Morgan, W. W., Keenan, P. C., & Kellman, E. 1943, *An Atlas of Stellar Spectra, with an Outline of Spectral Classification* (Chicago: Univ. Chicago Press)
- Morgan, W. W., Sharpless, S., & Osterbrock, D. 1952, *AJ*, 57, 3
- Motohara, K., et al. 2002, *PASJ*, 54, 315
- Nakajima, T., Oppenheimer, B. R., Kulkarni, S. R., Golimowski, D. A., Matthews, K., & Durrance, S. T. 1995, *Nature*, 378, 463
- Nakajima, T., Tsuji, T., Tamura, M., & Yamashita, T. 2000, *PASJ*, 52, 87
- Nakajima, T., Tsuji, T., & Yanagisawa, K. 2001, *ApJ*, 561, L119
- . 2004, *ApJ*, 607, 499
- Oppenheimer, B. R., Kulkarni, S. R., Matthews, K., & Nakajima, T. 1995, *Science*, 270, 1478
- Oppenheimer, B. R., Kulkarni, S. R., Matthews, K., van Kerkwijk, M. H. 1998, *ApJ*, 502, 932
- Rayner, J. T., Toomey, D. W., Onaka, P. M., Denault, A. J., Stahlberger, W. E., Vacca, W. D., Cushing, M. C., & Wang, S. 2003, *PASP*, 155, 362
- Reid, I. N., Burgasser, A. J., Cruz, K., Kirkpatrick, J. D., & Gizis, J. E. 2001, *AJ*, 121, 1710

- Reid, I. N., Hawley, S. L., & Gizis, J. E. 1995, *AJ*, 110, 1838
- Roellig, T. L., et al. 2004, *ApJS*, 154, 418
- Rountree, J., & Sonneborn, G. 1991, *ApJ*, 369, 515
- Saumon, D., Bergeron, P., Lunine, J. I., Hubbard, W. B., & Burrows, A. 1994, *ApJ*, 424, 333
- Scholz, R.-D., McCaughrean, M. J., Lodieu, N., & Kuhlbrodt, B. 2003, *A&A*, 398, L29
- Secchi, A. 1866, *CR Acad. Sci. Paris*, 63, 621
- Simons, D. A., & Tokunaga, A. T. 2002, *PASP*, 114, 169
- Stephens, D. C., & Leggett, S. K. 2004, *PASP*, 116, 9
- Strauss, M. A., et al. 1999, *ApJ*, 522, L61
- Testi, L., et al. 2001, *ApJ*, 522, L147
- Tinney, C. G., Burgasser, A. J., & Kirkpatrick, J. D. 2003, *AJ*, 126, 975
- Tinney, C. G., Burgasser, A. J., Kirkpatrick, J. D., & McElwain, M. W. 2005, *AJ*, in press
- Tinney, C. G., Delfosse, X., Forveille, T., & Allard, F. 1998, *A&A*, 338, 1066
- Tinney, C. G., & Tolley, A. J. 1999, *MNRAS*, 304, 119
- Tokunaga, A. T., & Kobayashi, N. 1999, *AJ*, 117, 1010
- Tokunaga, A. T., Simons, D. A., & Vacca, W. D. 2002, *PASP*, 114, 180
- Tsuji, T. 2005, *ApJ*, 621, 1033
- Tsuji, T., Ohnaka, K., Aoki, W., & Nakajima, T. 1996, *A&A*, 308, L29
- Tsuji, T., & Nakajima, T. 2003, *ApJ*, 585, L151
- Tsvetanov, Z. I., et al. 2000, *ApJ*, 531, L61
- Vacca, W. D., Cushing, M. C., & Rayner, J. T. 2003, *PASP*, 155, 389
- Vrba, F. J., et al. 2004, *AJ*, 127, 2948
- Warren, S. 2002, *Proc. SPIE*, 4836, 313
- Wallace, L., & Hinkle, K. 1997, *ApJS*, 111, 445
- Wilson, J. C., Skrutskie, M. F., Colonna, M. R., Enos, A. T., Smith, J. D., Henderson, C. P., Gizis, J. E., Monet, D. G., & Houck, J. R. 2001a, *PASP*, 113, 227

Wilson, J. C., et al. 2001b, *AJ*, 122, 1989

Woitke, P., & Helling, C. 2003, *A&A*, 339, 297

—. 2004, *A&A*, 414, 335

Wright, G. S., Mountain, C. M., Bridger, A., Daly, P. N., Griffin, J. L., & Ramsay-Howat, S. K. 1993, *Proc. SPIE*, 1946, 547

York, D. G., et al. 2000, *AJ*, 120, 1579

Zapatero Osorio, M. R., Béjar, V. J. S., Martí, E. L., Rebolo, R., Barrado y Navascuès, D., Mundt, R., Eislöffel, J., & Caballero, J. A. 2002, *ApJ*, 578, 536

Table 1. Spectral Datasets Examined for T Dwarf Classification.

Instrument	$\lambda/\Delta\lambda$	Spectral Coverage	Number of Orders	Number of Sources	References
CTIO 4m OSIRIS	1200	1.1–2.4 μm	4	20 T, 0 L	1,2
IRTF SpeX (prism)^a	150	0.8–2.5	1	43 T, 2 L	3,4,5,6
IRTF SpeX (SXD)	1200	0.9–2.5 μm	4–6	8 T, 1 L	3,7
Keck NIRC	100	0.9–2.5 μm	1–2	17 T, 0 L	1,8,9
Keck NIRSPEC	2000	Various	1–6	17 T, 2 L	10,11
NTT ISAAC+SOFI	50	0.95–2.5 μm	2	1 T, 0 L	12
Palomar 1.5m CORMASS	300	0.8–2.4 μm	4	1 T, 0 L	13
Subaru CISCO	500	0.9–2.5 μm	3	2 T, 0 L	14
Subaru IRCS	330	1.2–2.4 μm	3	1 T, 0 L	15
UKIRT CGS4^a	400	Various	1–4	39 T, 2 L	16,17,18,19,20,21,22
VLT NAOS-CONICA	1000	1.5–1.85 μm	1	2 T, 0 L	23

^aPrimary classification spectral sample.

References. — (1) B02; (2) Burgasser, McElwain, & Kirkpatrick (2003); (3) Burgasser et al. (2004a); (4) Cruz et al. (2004); (5) Burgasser, Burrows & Kirkpatrick (2005); (6) Burgasser et al., in prep.; (7) Cushing, Rayner & Vacca (2005); (8) Oppenheimer et al. (1995); (9) Zapatero Osorio et al. (2002); (10) McLean et al. (2003); (11) Liu et al. (2002); (12) Cuby et al. (1999); (13) Burgasser et al. (2000c); (14) Nakajima et al. (2004); (15) Nakajima et al. (2001); (16) Geballe et al. (1996); (17) Strauss et al. (1999); (18) Tsvetanov et al. (2000); (19) Leggett et al. (2000); (20) Geballe et al. (2001); (21) G02; (22) Knapp et al. (2004); (23) McCaughrean et al. (2004)

Note. — OSIRIS (Ohio State InfraRed Imager/Spectrometer): Depoy et al. (1993); SpeX: Rayner et al. (2003); NIRC (Near InfraRed Camera): Matthews & Soifer (1994); NIRSPEC (Near-IR Spectrometer): McLean et al. (1998, 2000); ISAAC (Infrared Spectrometer and Array Camera): Moorwood (1997); SOFI (Son of Isaac): Moorwood, Cuby & Lidman (1998); CORMASS (Cornell Massachusetts Slit Spectrograph): Wilson et al. (2001a); CISCO (Cooled Infrared Spectrograph and Camera for OHS): Motohara et al. (2002); IRCS (Infrared Camera and Spectograph): Kobayashi et al. (2000); CGS4 (Cooled Grating Spectrometer 4): Wright et al. (1993); NAOS/CONICA: Lenzen et al. (1998)

Table 2. T Dwarf Spectral Standards.

Name (1)	NIR SpT (2)	MKO Photometry ^a				d (pc) ^b (7)	Spectral Sample ^c (8)
		<i>J</i> (3)	<i>J</i> – <i>H</i> (4)	<i>H</i> – <i>K</i> (5)	<i>K</i> – <i>L'</i> (6)		
Primary Standards							
SDSS J120747.17+024424.8	T0	15.38±0.03	0.75±0.04	0.47±0.04	1.54±0.06	...	1
SDSS J083717.21–000018.0	T1	16.90±0.05	0.69±0.07	0.23±0.07	...	29±12	1,2,3
SDSS J125453.90–012247.4	T2	14.66±0.03	0.53±0.04	0.29±0.04	1.59±0.06	13.7±0.4	1,2,4,5,6,7
2MASS J12095613–1004008	T3	15.55±0.03	0.31±0.04	0.07±0.04	1,2
2MASS J22541892+3123498	T4	15.01±0.03	0.06±0.04	–0.08±0.04	1.79±0.06	...	1,2,3,5,7
2MASS J15031961+2525196	T5	13.55±0.03	–0.35±0.04	–0.09±0.04	2.08±0.06	...	2,4
SDSS J162414.37+002915.6	T6	15.20±0.03	–0.28±0.04	–0.13±0.04	2.01±0.05	11.00±0.15	1,2,5,7
2MASS J07271824+1710012	T7	15.19±0.03	–0.48±0.04	–0.02±0.04	2.01±0.06	9.09±0.17	1,2,3,5,7
2MASS J04151954–0935066	T8	15.32±0.03	–0.38±0.04	–0.13±0.04	2.55±0.06	5.57±0.10	1,2,3,5,7
Alternate Standards							
SDSS J042348.57–041403.5AB	T0	14.30±0.03	0.79±0.04	0.55±0.04	1.51±0.06	15.2±0.5	1,5,7
SDSS J015141.69+124429.6	T1	16.25±0.05	0.71±0.07	0.36±0.07	1.64±0.07	21.3±1.4	1,2,5
SDSS J102109.69–030420.1AB	T3	15.88±0.03	0.47±0.04	0.15±0.04	1.62±0.07	29±4	1,2,5
2MASS J07554795+2212169	T5	15.46±0.03	–0.24±0.04	–0.16±0.04	1
2MASS J15530228+1532369AB	T7	15.34±0.03	–0.42±0.04	–0.19±0.04	3,5,7

^aMKO *JHKL'* photometry from Strauss et al. (1999); Leggett et al. (2000, 2002b); G02; Golimowski et al. (2004); and Knapp et al. (2004).

^bParallax measurements from Dahn et al. (2002); Tinney, Burgasser, & Kirkpatrick (2003); and Vrba et al. (2004).

^cSpectral samples as follows: (1) UKIRT CGS4; (2) IRTF SpeX; (3) Keck NIRC; (4) IRTF SpeX cross-dispersed mode; (5) Keck NIRSPEC; (6) Subaru CISCO; (7) CTIO OSIRIS. See Table 1.

Table 3. Definitions of Near Infrared Spectral Indices.

Index (1)	Numerator Range ^a (2)	Denominator Range ^a (3)	Feature (4)
H₂O-J	1.140–1.165	1.260–1.285	1.15 μm H ₂ O
CH₄-J	1.315–1.340	1.260–1.285	1.32 μm CH ₄
H₂O-H	1.480–1.520	1.560–1.600	1.4 μm H ₂ O
CH₄-H	1.635–1.675	1.560–1.600	1.65 μm CH ₄
H ₂ O-K	1.975–1.995	2.080–2.100	1.9 μm H ₂ O
CH₄-K	2.215–2.255	2.080–2.120	2.2 μm CH ₄
K/J	2.060–2.100	1.250–1.290	<i>J</i> – <i>K</i> color

^aWavelength range (in microns) over which flux density (f_λ) is integrated.

Note. — Primary classification indices are listed in bold-face type.

Table 4. Near Infrared Spectral Indices for T Dwarf Spectral Standards.

Name (1)	NIR SpT (2)	H ₂ O-J (3)	CH ₄ -J (4)	H ₂ O-H (5)	CH ₄ -H (6)	CH ₄ -K (7)
SpeX Prism Data						
2MASS 1632+1904	L8 ^a	0.706	0.735	0.705	1.077	0.881
SDSS 0423–0414 ^b	T0	0.630	0.644	0.621	0.985	0.820
SDSS 0837–0000	T1	0.572	0.614	0.539	0.982	0.693
SDSS 1254–0122	T2	0.474	0.583	0.474	0.917	0.585
2MASS 1209–1004	T3	0.413	0.516	0.453	0.717	0.496
2MASS 2254+3123	T4	0.369	0.506	0.389	0.581	0.305
2MASS 1503+2525	T5	0.240	0.356	0.345	0.393	0.200
SDSS 1624+0029	T6	0.154	0.354	0.280	0.301	0.149
2MASS 0727+1710	T7	0.085	0.238	0.224	0.181	0.062
2MASS 0415–0935	T8	0.041	0.182	0.183	0.104	0.050
CGS4 Data ^c						
2MASS 1632+1904	L8 ^a	0.701	0.722	0.705	1.036	0.888
2MASS 0310+1648	L9 ^a	0.675	0.736	0.645	1.064	0.786
SDSS 1207+0244	T0	0.628	0.635	0.597	0.944	0.812
SDSS 0837–0000	T1	0.646	0.647	0.586	0.936	0.689
SDSS 1254–0122	T2	0.501	0.557	0.491	0.870	0.564
2MASS 1209–1004	T3	0.439	0.518	0.462	0.687	0.495
2MASS 2254+3123	T4	0.411	0.487	0.416	0.547	0.302
2MASS 1503+2525	T5	0.239	0.387	0.332	0.381	0.200
SDSS 1624+0029	T6	0.156	0.306	0.320	0.318	0.158
2MASS 0727+1710	T7	0.090	0.238	0.227	0.168	0.060
2MASS 0415–0935	T8	0.030	0.168	0.173	0.105	0.043

^aLate L dwarf comparison source.

^bAlternate standard.

^cWith the exception of SpeX cross-dispersed data for 2MASS 1503+2525 (Burgasser et al. 2004a).

Table 5. Numerical Ranges of Near Infrared Spectral Indices for T Dwarf Subtypes.

NIR SpT (1)	H ₂ O-J (2)	CH ₄ -J (3)	H ₂ O-H (4)	CH ₄ -H (5)	CH ₄ -K (6)
T0	...	0.73-0.78	0.60–0.66	0.97–1.00	0.75–0.85
T1	> 0.55	0.67-0.73	0.53–0.60	0.92–0.97	0.63–0.75
T2	0.45–0.55	0.58-0.67	0.46–0.53	0.80–0.92	0.55–0.63
T3	0.38–0.45	0.52-0.58	0.43–0.46	0.60–0.80	0.35–0.55
T4	0.32–0.38	0.45-0.52	0.37–0.43	0.48–0.60	0.24–0.35
T5	0.18–0.32	0.36-0.45	0.32–0.37	0.36–0.48	0.18–0.24
T6	0.13–0.18	0.28-0.36	0.26–0.32	0.25–0.36	0.13–0.18
T7	0.07–0.13	0.21-0.28	0.20–0.26	0.15–0.25	< 0.13
T8	0.02–0.07	0.15-0.21	0.14–0.20	0.07–0.15	...

Table 6. Spectral Indices and Classifications for SpeX Prism Spectra.

Name (1)	H ₂ O-J (2)	CH ₄ -J (3)	H ₂ O-H (4)	CH ₄ -H (5)	CH ₄ -K (6)	H ₂ O-K (7)	K/J (8)	Derived NIR SpT		
								Direct (9)	Ind 1 (10)	Ind 2 (11)
2M 1632+1904	0.706 (L8.0/-)	0.735 (L8.0/T0.0)	0.705 (L8.0/-)	1.077 (-/-)	0.881 (L8.0/-)	0.696	0.743	L8.0	L8.0	...
DE 0255-4700	0.671 (L8.0/-)	0.633 (T0.5/T2.0)	0.688 (L8.0/-)	1.030 (-/-)	0.835 (T0.0/T0.0)	0.691	0.603	L9.0	L9.0:	...
SD 0423-0414	0.630 (T0.0/-)	0.644 (T0.0/T2.0)	0.621 (T0.0/T0.0)	0.985 (T0.0/T0.0)	0.820 (T0.0/T0.0)	0.678	0.477	T0.0	T0.0	T0.5:
SD 0151+1244	0.654 (L9.5/-)	0.621 (T1.0/T2.0)	0.633 (T0.0/T0.0)	0.951 (T1.5/T1.0)	0.689 (T1.0/T1.0)	0.614	0.429	T0.5	T0.5	T1.0
SD 0837-0000	0.573 (T1.0/-)	0.616 (T1.0/T2.0)	0.560 (T0.5/T1.0)	0.977 (T1.0/T0.5)	0.754 (T0.5/T0.5)	0.608	0.400	T1.0	T1.0	T1.0
	0.572 (T1.0/-)	0.614 (T1.0/T2.0)	0.539 (T1.0/T1.5)	0.982 (T1.0/T0.0)	0.693 (T1.0/T1.0)	0.594	0.411	T1.0	T1.0	T1.0
2M 2139+0220	0.423 (T3.0/T3.0)	0.503 (T4.0/T4.0)	0.475 (T2.0/T2.5)	1.026 (-/-)	0.685 (T1.0/T1.0)	0.582	0.408	T1.5	T2.5:	T2.5:
	0.410 (T3.0/T3.0)	0.634 (T0.5/T2.0)	0.455 (T3.0/T2.5)	1.076 (-/-)	0.687 (T1.0/T1.0)	0.561	0.392	T1.5	T2.0:	T2.0
2M 0518-2828	0.438 (T2.5/T2.5)	0.556 (T2.5/T3.0)	0.620 (T0.0/T0.0)	0.831 (T2.5/T2.0)	0.816 (T0.0/T0.0)	0.724	0.517	T1.0p	T1.5:	T1.5:
2M 0949-1545	0.588 (T0.5/-)	0.583 (T2.0/T2.5)	0.612 (T0.0/T0.5)	0.812 (T2.5/T2.5)	0.421 (T3.5/T3.0)	0.549	0.328	T2.0	T1.5:	T2.0:
	0.570 (T1.0/-)	0.615 (T1.0/T2.0)	0.601 (T0.0/T0.5)	0.819 (T2.5/T2.5)	0.447 (T3.5/T3.0)	0.581	0.341	T2.0	T1.5:	T2.0:
2M 1122-3512	0.526 (T1.5/T1.5)	0.592 (T1.5/T2.5)	0.521 (T1.5/T1.5)	0.784 (T2.5/T2.5)	0.497 (T3.0/T3.0)	0.561	0.287	T2.0	T2.0	T2.0
SD 1254-0122	0.474 (T2.0/T2.5)	0.583 (T2.0/T2.5)	0.474 (T2.0/T2.5)	0.917 (T2.0/T1.5)	0.585 (T2.0/T2.0)	0.552	0.365	T2.0	T2.0	T2.0
SD 1750+4222	0.519 (T1.5/T2.0)	0.646 (T0.0/T2.0)	0.538 (T1.0/T1.5)	0.913 (T2.0/T1.5)	0.631 (T1.5/T1.5)	0.616	0.369	T2.0	T1.0	T1.5
SD 1021-0304	0.376 (T4.0/T3.5)	0.486 (T4.0/T4.0)	0.448 (T3.0/T3.0)	0.712 (T3.0/T3.0)	0.518 (T3.0/T2.5)	0.538	0.289	T3.0	T3.5	T3.0
2M 1209-1004	0.408 (T3.0/T3.0)	0.502 (T4.0/T4.0)	0.441 (T3.0/T3.0)	0.699 (T3.0/T3.0)	0.473 (T3.0/T3.0)	0.548	0.274	T3.0	T3.0	T3.0
	0.413 (T3.0/T3.0)	0.516 (T3.0/T3.5)	0.453 (T3.0/T2.5)	0.717 (T3.0/T3.0)	0.496 (T3.0/T3.0)	0.519	0.264	T3.0	T3.0	T3.0
SD 1750+1759	0.469 (T2.0/T2.5)	0.530 (T3.0/T3.5)	0.444 (T3.0/T3.0)	0.663 (T3.5/T3.0)	0.349 (T4.0/T3.5)	0.530	0.226	T3.5	T3.0	T3.0
SD 0207+0000	0.303 (T4.5/T4.5)	0.481 (T4.0/T4.0)	0.372 (T4.5/T4.5)	0.540 (T4.0/T4.0)	0.234 (T4.5/T4.5)	0.455	0.232	T4.0	T4.5	T4.5
2M 2151-4853	0.327 (T4.5/T4.5)	0.465 (T4.5/T4.5)	0.372 (T4.5/T4.5)	0.592 (T4.0/T3.5)	0.294 (T4.0/T4.0)	0.473	0.196	T4.0	T4.5	T4.0
2M 2254+3123	0.369 (T4.0/T3.5)	0.506 (T4.0/T4.0)	0.389 (T4.0/T4.0)	0.581 (T4.0/T3.5)	0.305 (T4.0/T4.0)	0.482	0.239	T4.0	T4.0	T4.0
SD 0000+2554	0.325 (T4.5/T4.5)	0.417 (T4.5/T5.0)	0.373 (T4.5/T4.5)	0.538 (T4.0/T4.0)	0.259 (T4.5/T4.5)	0.474	0.198	T4.5	T4.5	T4.5
2M 0559-1404	0.343 (T4.0/T4.0)	0.443 (T4.5/T4.5)	0.400 (T4.0/T4.0)	0.476 (T4.5/T4.5)	0.239 (T4.5/T4.5)	0.494	0.188	T4.5	T4.5	T4.5
2M 0407+1514	0.236 (T5.0/T5.0)	0.397 (T4.5/T5.0)	0.341 (T5.0/T5.0)	0.367 (T5.5/T5.5)	0.161 (T6.0/T6.0)	0.423	0.205	T5.0	T5.0	T5.5
2M 0755+2212	0.238 (T5.0/T5.0)	0.379 (T5.0/T5.5)	0.350 (T5.0/T5.0)	0.378 (T5.0/T5.5)	0.224 (T5.0/T5.0)	0.476	0.155	T5.0	T5.0	T5.0
2M 1503+2525	0.240 (T5.0/T5.0)	0.356 (T5.0/T5.5)	0.345 (T5.0/T5.0)	0.393 (T5.0/T5.0)	0.200 (T5.0/T5.0)	0.450	0.151	T5.0	T5.0	T5.0
2M 1828-4849	0.183 (T5.5/T5.5)	0.347 (T6.0/T5.5)	0.310 (T5.5/T5.5)	0.369 (T5.5/T5.5)	0.197 (T5.0/T5.0)	0.459	0.170	T5.0	T5.5	T5.5
2M 1901+4718	0.285 (T4.5/T4.5)	0.420 (T4.5/T5.0)	0.355 (T5.0/T5.0)	0.435 (T5.0/T5.0)	0.237 (T4.5/T4.5)	0.497	0.171	T5.0	T4.5	T5.0
SD 2124+0059	0.245 (T5.0/T5.0)	0.448 (T4.5/T4.5)	0.337 (T5.0/T5.0)	0.399 (T5.0/T5.0)	0.193 (T5.0/T5.5)	0.415	0.191	T5.0	T5.0	T5.0
2M 2331-4718	0.196 (T5.5/T5.5)	0.394 (T4.5/T5.0)	0.325 (T5.5/T5.5)	0.450 (T4.5/T4.5)	0.205 (T5.0/T5.0)	0.445	0.205	T5.0	T5.0	T5.0
2M 2339+1352	0.243 (T5.0/T5.0)	0.380 (T5.0/T5.5)	0.325 (T5.5/T5.5)	0.449 (T4.5/T5.0)	0.234 (T4.5/T4.5)	0.448	0.163	T5.0	T5.0	T5.0
2M 2356-1553	0.237 (T5.0/T5.0)	0.412 (T4.5/T5.0)	0.331 (T5.0/T5.5)	0.357 (T5.5/T5.5)	0.159 (T6.0/T6.0)	0.408	0.197	T5.0	T5.0	T5.5

Table 6—Continued

Name (1)	H ₂ O-J (2)	CH ₄ -J (3)	H ₂ O-H (4)	CH ₄ -H (5)	CH ₄ -K (6)	H ₂ O-K (7)	K/J (8)	Derived NIR SpT		
								Direct (9)	Ind 1 (10)	Ind 2 (11)
SD 1110+0116	0.152 (T6.0/T6.0)	0.333 (T6.0/T6.0)	0.303 (T5.5/T6.0)	0.335 (T5.5/T5.5)	0.175 (T5.5/T5.5)	0.402	0.217	T5.5	T5.5	T6.0
2M 1231+0847	0.181 (T5.5/T5.5)	0.343 (T6.0/T5.5)	0.271 (T6.0/T6.5)	0.359 (T5.5/T5.5)	0.163 (T5.5/T6.0)	0.372	0.157	T5.5	T5.5	T6.0
2M 0243-2453	0.145 (T6.0/T6.0)	0.324 (T6.5/T6.0)	0.297 (T5.5/T6.0)	0.334 (T5.5/T5.5)	0.160 (T6.0/T6.0)	0.438	0.197	T6.0	T6.0	T6.0
2M 0937+2931	0.151 (T6.0/T6.0)	0.330 (T6.0/T6.0)	0.316 (T5.5/T5.5)	0.305 (T6.0/T6.0)	0.206 (T5.0/T5.0)	0.514	0.076	T6.0p	T5.5	T5.5
2M 1225-2739	0.171 (T6.0/T5.5)	0.331 (T6.0/T6.0)	0.286 (T6.0/T6.0)	0.325 (T5.5/T6.0)	0.180 (T5.5/T5.5)	0.441	0.147	T6.0	T6.0	T6.0
SD 1624+0029	0.167 (T6.0/T6.0)	0.339 (T6.0/T6.0)	0.314 (T5.5/T5.5)	0.311 (T6.0/T6.0)	0.141 (T6.0/T6.5)	0.416	0.156	T6.0	T6.0	T6.0
	0.154 (T6.0/T6.0)	0.354 (T6.0/T5.5)	0.280 (T6.0/T6.0)	0.301 (T6.0/T6.0)	0.149 (T6.0/T6.0)	0.418	0.142	T6.0	T6.0	T6.0
2M 2228-4310	0.157 (T6.0/T6.0)	0.328 (T6.0/T6.0)	0.293 (T6.0/T6.0)	0.262 (T6.5/T6.5)	0.116 (T6.5/-)	0.352	0.204	T6.0	T6.0	T6.0
2M 0034+0523	0.103 (T6.5/T7.0)	0.333 (T6.0/T6.0)	0.229 (T7.0/T7.0)	0.231 (T6.5/T6.5)	0.131 (T6.0/T6.5)	0.421	0.100	T6.5	T6.5	T6.5
SD 1346-0031	0.131 (T6.5/T6.5)	0.304 (T6.5/T6.0)	0.278 (T6.0/T6.0)	0.268 (T6.5/T6.5)	0.124 (T6.5/-)	0.421	0.156	T6.5	T6.5	T6.5
SD 1758+4633	0.101 (T7.0/T7.0)	0.302 (T6.5/T6.0)	0.247 (T6.5/T6.5)	0.250 (T6.5/T6.5)	0.101 (T6.5/-)	0.356	0.200	T6.5	T6.5	T6.5
2M 0050-3322	0.104 (T6.5/T7.0)	0.311 (T6.5/T6.0)	0.266 (T6.0/T6.5)	0.184 (T7.0/T7.0)	0.070 (T7.0/-)	0.352	0.180	T7.0	T6.5	T6.5
2M 0727+1710	0.085 (T7.0/T7.0)	0.238 (T7.0/T7.0)	0.224 (T7.0/T7.0)	0.181 (T7.0/T7.0)	0.062 (T7.0/-)	0.340	0.164	T7.0	T7.0	T7.0
2M 1114-2618	0.039 (T8.0/T8.0)	0.201 (T8.0/T7.5)	0.177 (T8.0/T8.0)	0.160 (T7.5/T7.5)	0.080 (T7.0/-)	0.498	0.076	T7.5	T7.5	T8.0
2M 1217-0311	0.066 (T7.5/T7.5)	0.221 (T7.5/T7.5)	0.207 (T7.5/T7.5)	0.139 (T8.0/T7.5)	0.055 (T8.0/-)	0.361	0.179	T7.5	T7.5	T7.5
Gl 570D	0.063 (T8.0/T7.5)	0.229 (T7.0/T7.0)	0.198 (T8.0/T7.5)	0.141 (T8.0/T7.5)	0.098 (T6.5/-)	0.350	0.116	T7.5	T7.5	T7.5
2M 0939-2448	0.032 (T8.0/T8.0)	0.228 (T7.0/T7.0)	0.162 (T8.0/T8.0)	0.135 (T8.0/T7.5)	0.124 (T6.5/-)	0.505	0.063	T8.0	T7.5	T8.0
	0.038 (T8.0/T8.0)	0.209 (T8.0/T7.5)	0.149 (T8.0/T8.0)	0.135 (T8.0/T7.5)	0.189 (T5.0/T5.5)	0.433	0.059	T8.0	T7.5:	T7.5:
2M 0415-0935	0.041 (T8.0/T8.0)	0.182 (T8.0/T8.0)	0.183 (T8.0/T8.0)	0.104 (T8.0/T8.0)	0.050 (T8.0/-)	0.311	0.131	T8.0	T8.0	T8.0

Note. — Index subtypes in parentheses determined by direct comparison to spectral standard ratios (Table 4) or spectral ratio ranges (Table 5); see § 4.2.2. Uncertain classifications are indicated by “:”; peculiar sources are indicated by “p”.

Table 7. Spectral Indices and Classifications for CGS4 Spectra.

Name (1)	H ₂ O-J (2)	CH ₄ -J (3)	H ₂ O-H (4)	CH ₄ -H (5)	CH ₄ -K (6)	H ₂ O-K (7)	K/J (8)	Derived NIR SpT		
								Direct (9)	Ind 1 (10)	Ind 2 (11)
2M 1632+1904	0.701 (L8.0/-)	0.722 (L8.0/T0.5)	0.705 (L8.0/-)	1.036 (-/-)	0.888 (L8.0/-)	0.700	0.769	L8.0	L8.0	...
2M 0310+1648	0.675 (L9.0/-)	0.736 (L9.0/T0.5)	0.645 (L9.0/T0.0)	1.064 (-/-)	0.786 (L9.0/T0.0)	0.667	0.683	L9.0	L9.0	...
SD 0423-0414	0.671 (L9.0/-)	0.663 (T1.0/T1.5)	0.620 (L9.5/T0.0)	0.959 (T0.0/T0.5)	0.820 (T0.0/T0.0)	0.670	0.493	T0.0	T0.0	T0.5
SD 1104+5548	0.657 (L9.0/L9.5)	0.947 (T0.0/T1.0)	0.855 (L8.0/-)	0.656	...	T0.0:	L9.0:	T0.5:
SD 1207+0244	0.628 (T0.0/-)	0.635 (T0.0/T2.0)	0.597 (T0.0/T0.5)	0.944 (T0.0/T1.0)	0.812 (T0.0/T0.0)	0.691	0.446	T0.0	T0.0	T1.0
SD 1516+0259	0.640 (L9.0/T0.0)	0.884 (T2.0/T2.0)	0.861 (L8.0/-)	0.751	...	T0.0:	L9.5::	T1.0:
SD 2047-0718	0.707 (L8.0/-)	0.675 (T1.0/T1.5)	0.652 (L9.0/L9.5)	0.930 (T1.0/T1.5)	0.847 (T0.0/L9.5)	0.670	0.514	T0.0:	T0.0:	T0.5:
SD 0151+1244	0.673 (L9.0/-)	0.658 (T1.0/T1.5)	0.586 (T1.0/T0.5)	0.950 (T0.0/T1.0)	0.697 (T1.0/T1.0)	0.634	0.421	T0.5	T0.5	T1.0
SD 0837-0000	0.646 (T1.0/-)	0.647 (T1.0/T2.0)	0.586 (T1.0/T0.5)	0.936 (T1.0/T1.0)	0.689 (T1.0/T1.0)	0.608	0.363	T1.0	T1.0	T1.0
SD 1632+4150	0.640 (T1.0/-)	0.628 (T0.0/T2.0)	0.532 (T1.5/T1.5)	0.868 (T2.0/T2.0)	0.556 (T2.0/T2.5)	0.648	0.330	T1.0:	T1.5	T2.0
SD 1157+0611	0.572 (T0.0/-)	0.579 (T2.0/T2.5)	0.474 (T2.5/T2.5)	0.936 (T1.0/T1.0)	0.695 (T1.0/T1.0)	0.619	0.420	T1.5	T1.5	T2.0
SD 0758+3247	0.409 (T4.0/T3.0)	0.557 (T2.0/T3.0)	0.471 (T2.5/T2.5)	0.900 (T1.5/T1.5)	0.632 (T1.5/T1.5)	0.539	0.359	T2.0	T2.5:	T2.5
SD 1254-0122	0.501 (T2.0/T2.0)	0.557 (T2.0/T3.0)	0.491 (T2.0/T2.0)	0.870 (T2.0/T2.0)	0.564 (T2.0/T2.5)	0.554	0.352	T2.0	T2.0	T2.5
SD 1521+0131	0.508 (T2.0/T2.0)	0.519 (T3.0/T3.5)	0.573 (T1.0/T1.0)	0.913 (T1.5/T1.5)	0.499 (T3.0/T3.0)	0.560	0.297	T2.0:	T2.0:	T2.0:
SD 1750+4222	0.574 (T0.0/-)	0.673 (T1.0/T1.5)	0.599 (T0.0/T0.5)	0.920 (T1.0/T1.5)	0.593 (T2.0/T2.0)	0.628	0.342	T2.0	T1.0	T1.5
2M 1209-1004	0.439 (T3.0/T2.5)	0.518 (T3.0/T3.5)	0.462 (T3.0/T2.5)	0.687 (T3.0/T3.0)	0.495 (T3.0/T3.0)	0.516	0.253	T3.0	T3.0	T3.0
SD 1021-0304	0.381 (T4.0/T3.5)	0.491 (T4.0/T4.0)	0.444 (T3.5/T3.0)	0.694 (T3.0/T3.0)	0.530 (T2.5/T2.5)	0.565	0.291	T3.0	T3.5	T3.0
SD 1750+1759	0.433 (T3.0/T2.5)	0.521 (T3.0/T3.5)	0.476 (T2.5/T2.5)	0.628 (T3.5/T3.5)	0.351 (T3.5/T3.5)	0.495	0.226	T3.5	T3.0	T3.0
2M 2254+3123	0.411 (T4.0/T3.0)	0.487 (T4.0/T4.0)	0.416 (T4.0/T3.5)	0.547 (T4.0/T4.0)	0.302 (T4.0/T4.0)	0.523	0.202	T4.0	T4.0	T3.5
SD 0000+2554	0.338 (T4.5/T4.0)	0.438 (T4.5/T4.5)	0.388 (T4.5/T4.0)	0.537 (T4.0/T4.0)	0.274 (T4.5/T4.0)	0.459	0.197	T4.0	T4.5	T4.0
2M 0559-1404	0.328 (T4.5/T4.5)	0.453 (T4.5/T4.5)	0.384 (T4.5/T4.5)	0.477 (T4.5/T4.5)	0.234 (T4.5/T4.5)	0.474	0.179	T4.5	T4.5	T4.5
SD 0207+0000	0.312 (T4.5/T4.5)	0.490 (T4.0/T4.0)	0.379 (T4.5/T4.5)	0.523 (T4.0/T4.0)	0.226 (T4.5/T4.5)	0.480	0.214	T4.5	T4.5	T4.5
SD 0830+0128	0.354 (T4.5/T5.0)	0.437 (T4.5/T5.0)	T4.5	T4.5	T5.0
SD 0926+5847	0.367 (T4.5/T3.5)	0.415 (T4.5/T5.0)	0.363 (T4.5/T4.5)	0.490 (T4.5/T4.5)	0.257 (T4.5/T4.5)	0.468	0.206	T4.5	T4.5	T4.5
2M 2339+1352	0.227 (T5.0/T5.0)	0.372 (T5.0/T5.5)	0.305 (T6.0/T5.5)	0.426 (T4.5/T5.0)	0.196 (T5.0/T5.0)	0.465	0.148	T5.0	T5.0	T5.0
SD 0741+2351	0.224 (T5.0/T5.0)	0.367 (T5.5/T5.5)	0.308 (T6.0/T5.5)	0.360 (T5.5/T5.5)	0.183 (T5.5/T5.5)	0.426	0.156	T5.0	T5.5	T5.5
SD 0742+2055	0.252 (T5.0/T5.0)	0.382 (T5.0/T5.5)	0.356 (T4.5/T5.0)	0.363 (T5.5/T5.5)	0.193 (T5.0/T5.5)	0.473	0.136	T5.0	T5.0	T5.5
SD 1110+0116	0.190 (T5.5/T5.5)	0.360 (T5.5/T5.5)	0.321 (T6.0/T5.5)	0.397 (T5.0/T5.0)	0.159 (T6.0/T6.0)	0.479	0.232	T5.0	T5.5	T5.5
SD 2124+0059	0.373 (T4.5/T4.5)	0.392 (T5.0/T5.0)	T5.0	T5.0	T5.0
2M 1231+0847	0.185 (T5.5/T5.5)	0.326 (T6.0/T6.0)	0.282 (T6.5/T6.0)	0.338 (T5.5/T5.5)	0.190 (T5.0/T5.5)	0.386	0.156	T5.5	T5.5	T5.5
2M 0937+2931	0.164 (T6.0/T6.0)	0.324 (T6.0/T6.0)	0.311 (T6.0/T5.5)	0.288 (T6.0/T6.0)	0.231 (T4.5/T4.5)	0.507	0.068	T6.0p	T5.5	T5.5
2M 1225-2739	0.185 (T5.5/T5.5)	0.301 (T6.0/T6.0)	0.323 (T5.5/T5.5)	0.301 (T6.0/T6.0)	0.125 (T6.5/-)	0.394	0.147	T6.0	T6.0	T6.0

Table 7—Continued

Name (1)	H ₂ O-J (2)	CH ₄ -J (3)	H ₂ O-H (4)	CH ₄ -H (5)	CH ₄ -K (6)	H ₂ O-K (7)	K/J (8)	Derived NIR SpT		
								Direct (9)	Ind 1 (10)	Ind 2 (11)
SD 1346-0031	0.159 (T6.0/T6.0)	0.232 (T7.0/T7.0)	0.290 (T6.5/T6.0)	0.265 (T6.5/T6.5)	0.114 (T6.5/-)	0.418	0.170	T6.0	T6.5	T6.5
SD 1624+0029	0.156 (T6.0/T6.0)	0.306 (T6.0/T6.0)	0.320 (T6.0/T5.5)	0.318 (T6.0/T6.0)	0.158 (T6.0/T6.0)	0.447	0.140	T6.0	T6.0	T6.0
2M 1047+2124	0.259 (T6.5/T6.5)	0.253 (T6.5/T6.5)	T6.5	T6.5	T6.5
SD 1758+4633	0.114 (T6.5/T7.0)	0.239 (T7.0/T7.0)	0.289 (T6.5/T6.0)	0.237 (T6.5/T6.5)	0.103 (T6.5/-)	0.414	0.160	T6.5	T6.5	T6.5
2M 0727+1707	0.090 (T7.0/T7.0)	0.238 (T7.0/T7.0)	0.227 (T7.0/T7.0)	0.168 (T7.0/T7.5)	0.060 (T7.0/-)	0.349	0.144	T7.0	T7.0	T7.0
Gl 229B	0.146 (T6.0/T6.0)	0.243 (T7.0/T7.0)	0.333 (T5.0/T5.0)	0.192 (T7.0/T7.0)	0.202 (T5.0/T5.0)	0.391	0.135	T7.0p	T6.0:	T6.0:
2M 1217-0311	0.082 (T7.0/T7.5)	0.221 (T7.0/T7.5)	0.232 (T7.0/T7.0)	0.146 (T7.5/T7.5)	0.058 (T7.0/-)	0.366	0.164	T7.5	T7.0	T7.5
Gl 570D	0.068 (T7.5/T7.5)	0.205 (T7.5/T7.5)	0.208 (T7.5/T7.5)	0.137 (T7.5/T7.5)	0.073 (T7.0/-)	0.368	0.105	T7.5	T7.5	T7.5
2M 0415-0935	0.030 (T8.0/T8.0)	0.168 (T8.0/T8.0)	0.173 (T8.0/T8.0)	0.105 (T8.0/T8.0)	0.043 (T8.0/-)	0.317	0.134	T8.0	T8.0	T8.0

Note. — Index subtypes in parentheses determined by direct comparison to spectral standard ratios (Table 4) or spectral ratio ranges (Table 5); see § 4.2.2. Uncertain classifications are indicated by “:”; peculiar sources are indicated by “p”.

Table 8. Spectral Indices and Classifications for NIRC Grism Spectra.

Name (1)	H ₂ O-J (2)	CH ₄ -J (3)	H ₂ O-H (4)	CH ₄ -H (5)	CH ₄ -K (6)	H ₂ O-K (7)	K/J (8)	Derived NIR SpT		
								Direct (9)	Ind 1 (10)	Ind 2 (11)
2M 0920+3517	0.761 (L8.0/-)	0.635 (T0.5/T2.0)	0.716 (L8.0/-)	0.964 (T1.5/T0.5)	0.860 (L8.0/-)	0.653	0.538	T0.0p	L9.0:	T1.5:
2M 2254+3123	0.453 (T2.5/T2.5)	0.366 (T5.0/T5.5)	0.425 (T3.5/T3.5)	0.558 (T4.0/T4.0)	0.266 (T4.5/T4.5)	0.549	0.191	T4.0	T4.0	T4.0:
2M 0559-1404	0.366 (T4.0/T3.5)	0.405 (T4.5/T5.0)	0.375 (T4.5/T4.5)	0.491 (T4.5/T4.5)	0.228 (T4.5/T4.5)	0.445	0.252	T4.5	T4.5	T4.5
	0.322 (T4.5/T4.5)	0.437 (T4.5/T4.5)	0.347 (T5.0/T5.0)	0.509 (T4.5/T4.5)	0.243 (T4.5/T4.5)	0.524	0.275	T4.5	T4.5	T4.5
2M 2339+1352	0.303 (T4.5/T4.5)	0.232 (T7.0/T7.0)	0.317 (T5.5/T5.5)	0.424 (T5.0/T5.0)	0.200 (T5.0/T5.0)	0.511	0.169	T5.0	T5.5	T5.5
2M 2356-1553	0.250 (T5.0/T5.0)	0.403 (T4.5/T5.0)	0.299 (T5.5/T6.0)	0.352 (T5.5/T5.5)	0.160 (T6.0/T6.0)	0.495	0.228	T5.5	T5.5	T5.5
2M 0243-2453	0.161 (T6.0/T6.0)	0.267 (T7.0/T6.5)	0.278 (T6.0/T6.0)	0.327 (T5.5/T6.0)	0.158 (T6.0/T6.0)	0.494	0.198	T6.0	T6.0	T6.0
2M 0937+2931	0.177 (T5.5/T5.5)	0.290 (T6.5/T6.5)	0.281 (T6.0/T6.0)	0.324 (T5.5/T6.0)	0.236 (T4.5/T4.5)	0.634	0.121	T6.0p	T5.5	T5.5
	0.181 (T5.5/T5.5)	0.282 (T6.5/T6.5)	0.314 (T5.5/T5.5)	0.296 (T6.0/T6.0)	0.214 (T5.0/T5.0)	0.577	0.097	T6.0p	T5.5	T5.5
S Ori 70	0.280 (T6.0/T6.0)	0.225 (T5.0/T4.5)	0.502	...	T6.0:	T5.5	T5.5:
2M 1047+2124	0.162 (T6.0/T6.0)	0.244 (T7.0/T7.0)	0.248 (T6.5/T6.5)	0.263 (T6.5/T6.5)	0.171 (T5.5/T5.5)	0.485	0.149	T6.5	T6.5	T6.5
	0.162 (T6.0/T6.0)	0.244 (T7.0/T7.0)	0.247 (T6.5/T6.5)	0.263 (T6.5/T6.5)	0.171 (T5.5/T5.5)	0.485	0.155	T6.5	T6.5	T6.5
2M 1237+6526	0.123 (T6.5/T6.5)	0.245 (T7.0/T7.0)	0.233 (T7.0/T7.0)	0.239 (T6.5/T6.5)	0.156 (T6.0/T6.0)	0.520	0.101	T6.5	T6.5	T6.5
SD 1346-0031	0.146 (T6.0/T6.0)	0.267 (T7.0/T6.5)	0.271 (T6.0/T6.5)	0.273 (T6.0/T6.5)	0.161 (T6.0/T6.0)	0.485	0.182	T6.5	T6.0	T6.5
2M 0727+1710	0.104 (T6.5/T7.0)	0.223 (T7.5/T7.5)	0.218 (T7.0/T7.0)	0.196 (T7.0/T7.0)	0.100 (T6.5/-)	0.385	0.147	T7.0	T7.0	T7.0
2M 1217-0311	0.085 (T7.0/T7.0)	0.177 (T8.0/T8.0)	0.229 (T7.0/T7.0)	0.154 (T7.5/T7.5)	0.096 (T6.5/-)	0.422	0.205	T7.0	T7.0	T7.5
2M 1553+1532	0.112 (T6.5/T7.0)	0.185 (T8.0/T8.0)	0.223 (T7.0/T7.0)	0.192 (T7.0/T7.0)	0.093 (T6.5/-)	0.435	0.194	T7.0	T7.0	T7.5
Gl 229B	...	0.176 (T8.0/T8.0)	0.380 (T4.0/T4.5)	0.239 (T6.5/T6.5)	0.197 (T5.0/T5.0)	...	0.126	T7.0p	T6.0:	T6.0:
Gl 570D	0.071 (T7.5/T7.5)	0.195 (T8.0/T8.0)	0.177 (T8.0/T8.0)	0.153 (T7.5/T7.5)	0.074 (T7.0/-)	0.421	0.161	T7.5	T7.5	T8.0
2M 0415-0935	0.061 (T8.0/T7.5)	0.177 (T8.0/T8.0)	0.157 (T8.0/T8.0)	0.117 (T8.0/T8.0)	0.098 (T6.5/-)	0.353	0.209	T8.0	T7.5	T8.0
	0.054 (T8.0/T8.0)	0.186 (T8.0/T8.0)	0.162 (T8.0/T8.0)	0.114 (T8.0/T8.0)	0.064 (T7.0/-)	0.370	0.167	T8.0	T8.0	T8.0

Note. — Index subtypes in parentheses determined by direct comparison to spectral standard ratios (Table 4) or spectral ratio ranges (Table 5); see § 4.2.2. Uncertain classifications are indicated by “:”; peculiar sources are indicated by “p”.

Table 9. Spectral Indices and Classifications for SpeX Cross Dispersed Spectra.

Name (1)	H ₂ O-J (2)	CH ₄ -J (3)	H ₂ O-H (4)	CH ₄ -H (5)	CH ₄ -K (6)	H ₂ O-K (7)	K/J (8)	Derived NIR SpT		
								Direct (9)	Ind 1 (10)	Ind 2 (11)
DE 0255-4700	0.695 (L8.0/-)	0.718 (L8.0/T0.5)	0.684 (L8.0/-)	1.007 (-/-)	0.848 (T0.0/T0.0)	0.686	0.603	L9.0	L8.5:	...
SD 1254-0122	0.501 (T2.0/T2.0)	0.582 (T1.5/T2.5)	0.494 (T2.0/T2.0)	0.880 (T2.0/T2.0)	0.576 (T2.0/T2.0)	0.567	0.327	T2.0	T2.0	T2.0
2M 0559-1404	0.342 (T4.5/T4.0)	0.454 (T4.5/T4.5)	0.388 (T4.5/T4.0)	0.472 (T4.5/T4.5)	0.239 (T4.5/T4.5)	0.468	0.192	T4.5	T4.5	T4.5
2M 1503+2525	0.239 (T5.0/T5.0)	0.387 (T5.0/T5.0)	0.332 (T5.0/T5.5)	0.381 (T5.0/T5.5)	0.200 (T5.0/T5.0)	0.436	0.151	T5.0	T5.0	T5.0
2M 1901+4718	0.305 (T4.5/T4.5)	0.444 (T4.5/T4.5)	0.354 (T4.5/T5.0)	0.437 (T4.5/T5.0)	0.261 (T4.5/T4.5)	0.504	0.172	T5.0	T4.5	T4.5
2M 2331-4718	0.235 (T5.0/T5.0)	0.377 (T5.0/T5.5)	0.332 (T5.0/T5.5)	0.424 (T4.5/T5.0)	0.225 (T5.0/T4.5)	0.522	0.208	T5.0	T5.0	T5.0
2M 1231+0847	0.194 (T5.5/T5.5)	0.353 (T5.5/T5.5)	0.278 (T6.5/T6.0)	0.347 (T5.5/T5.5)	0.161 (T6.0/T6.0)	0.401	0.156	T5.5	T6.0	T5.5
2M 1828-4849	0.175 (T6.0/T5.5)	0.347 (T5.5/T5.5)	0.310 (T6.0/T5.5)	0.360 (T5.5/T5.5)	0.197 (T5.0/T5.0)	0.515	0.166	T5.5	T5.5	T5.5
2M 0034+0523	0.106 (T7.0/T7.0)	0.266 (T6.5/T6.5)	0.242 (T7.0/T7.0)	0.217 (T6.5/T7.0)	0.153 (T6.0/T6.0)	0.457	0.100	T6.5	T6.5	T6.5

Note. — Index subtypes in parentheses determined by direct comparison to spectral standard ratios (Table 4) or spectral ratio ranges (Table 5); see § 4.2.2. Uncertain classifications are indicated by “.”; peculiar sources are indicated by “p”.

Table 10. Spectral Indices and Classifications for NIRSPEC Spectra.

Name (1)	H ₂ O-J (2)	CH ₄ -J (3)	H ₂ O-H (4)	CH ₄ -H (5)	CH ₄ -K (6)	H ₂ O-K (7)	K/J (8)	Derived NIR SpT		
								Direct (9)	Ind 1 (10)	Ind 2 (11)
2M 1632+1904	0.649 (T1.0/-)	0.723 (L8.0/T0.5)	0.696 (L8.0/-)	1.042 (-/-)	0.892 (L8.0/-)	0.683	0.898	L8.0	L8.5:	...
2M 0310+1648	...	0.679 (T1.0/T1.5)	L9.0	T1.0:	T1.5:
Gl 337CD	0.632 (T0.0/-)	0.712 (L8.0/T1.0)	0.697 (L8.0/-)	0.973 (T0.0/T0.5)	0.789 (L9.0/T0.0)	0.685	0.712	T0.0	L9.0:	T0.5
SD 0423-0414	0.605 (T0.0/-)	0.656 (T1.0/T1.5)	0.615 (L9.5/T0.0)	0.956 (T0.0/T1.0)	0.826 (T0.0/T0.0)	0.658	0.558	T0.0	T0.0	T0.5
SD 0151+1244	...	0.655 (T1.0/T1.5)	T1.0	T1.0:	T1.5:
SD 0837-0000	...	0.641 (T0.0/T2.0)	0.569 (T1.0/T1.0)	0.991 (L8.0/T0.0)	0.710 (T1.0/T1.0)	0.599	0.306	T1.0	T0.0:	T1.0
SD 1254-0122	0.465 (T2.5/T2.5)	0.554 (T2.0/T3.0)	0.474 (T2.5/T2.5)	0.886 (T2.0/T2.0)	0.573 (T2.0/T2.0)	0.548	0.294	T2.0	T2.0	T2.5
SD 1021-0304	...	0.503 (T3.5/T4.0)	T3.0	T3.5:	T4.0:
SD 1750+1759	...	0.541 (T2.5/T3.0)	T3.5	T2.5:	T3.0:
2M 2254+3123	0.330 (T4.5/T4.5)	0.476 (T4.0/T4.0)	0.403 (T4.0/T4.0)	0.551 (T4.0/T4.0)	0.264 (T4.5/T4.5)	0.500	0.167	T4.0	T4.0	T4.0
2M 0559-1404	0.320 (T4.5/T4.5)	0.458 (T4.5/T4.5)	0.384 (T4.5/T4.5)	0.474 (T4.5/T4.5)	0.233 (T4.5/T4.5)	0.465	0.218	T4.5	T4.5	T4.5
SD 0926+5847	...	0.428 (T4.5/T4.5)	T4.5	T4.5:	T4.5: ₃₅
2M 2356-1553	0.194 (T5.5/T5.5)	0.413 (T4.5/T5.0)	0.364 (T4.5/T4.5)	0.333 (T6.0/T5.5)	0.168 (T6.0/T5.5)	0.424	0.137	T5.5	T5.5	T5.0 ₃₅
SD 1624+0029	...	0.318 (T6.0/T6.0)	T6.0	T6.0:	T6.0: ₃₅
2M 0727+1710	...	0.236 (T7.0/T7.0)	T7.0	T7.0:	T7.0:
2M 1237+6526	0.129 (T6.5/T6.5)	0.265 (T6.5/T6.5)	T7.0	T6.5	T6.5
2M 1553+1532	...	0.244 (T7.0/T7.0)	T7.0	T7.0:	T7.0:
Gl 570D	0.058 (T8.0/T7.5)	0.204 (T7.5/T7.5)	0.207 (T7.5/T7.5)	0.143 (T7.5/T7.5)	0.074 (T7.0/-)	0.353	0.081	T7.5	T7.5	T7.5
2M 0415-0935	0.038 (T8.0/T8.0)	0.171 (T8.0/T8.0)	...	0.119 (T8.0/T8.0)	0.090 (T6.5/-)	0.339	0.175	T8.0	T7.5	T8.0

Note. — Index subtypes in parentheses determined by direct comparison to spectral standard ratios (Table 4) or spectral ratio ranges (Table 5); see § 4.2.2. Uncertain classifications are indicated by “:”; peculiar sources are indicated by “p”.

Table 11. Spectral Indices and Classifications for OSIRIS Spectra.

Name (1)	H ₂ O-J (2)	CH ₄ -J (3)	H ₂ O-H (4)	CH ₄ -H (5)	CH ₄ -K (6)	H ₂ O-K (7)	K/J (8)	Derived NIR SpT		
								Direct (9)	Ind 1 (10)	Ind 2 (11)
SD 0423-0414	...	0.628 (T0.0/T2.0)	0.615 (L9.5/T0.0)	0.923 (T1.0/T1.5)	0.822 (T0.0/T0.0)	0.687	0.470	T0.0	T0.0	T1.0:
SD 1254-0122	...	0.554 (T2.0/T3.0)	0.483 (T2.5/T2.0)	0.855 (T2.0/T2.0)	0.540 (T2.5/T2.5)	0.507	0.412	T2.0	T2.5	T2.5
2M 2254+3123	...	0.439 (T4.5/T4.5)	0.372 (T4.5/T4.5)	0.520 (T4.0/T4.0)	...	0.386	0.204	T4.0	T4.5	T4.5
2M 0559-1404	...	0.371 (T5.0/T5.5)	0.320 (T6.0/T5.5)	0.402 (T5.0/T5.0)	0.216 (T5.0/T5.0)	0.558	0.215	T4.5	T5.5	T5.5
2M 1534-2952	...	0.364 (T5.5/T5.5)	0.341 (T5.0/T5.0)	0.397 (T5.0/T5.0)	0.195 (T5.0/T5.0)	0.452	0.145	T5.0	T5.0	T5.0
2M 0243-2453	...	0.500 (T3.5/T4.0)	0.203 (T7.5/T7.5)	0.247 (T6.5/T6.5)	...	0.549	0.231	T6.0:	T6.0:	T6.0:
2M 0937+2931	...	0.311 (T6.0/T6.0)	0.268 (T6.5/T6.5)	0.261 (T6.5/T6.5)	0.089	T6.0p	T6.5	T6.5
2M 1225-2739	...	0.306 (T6.0/T6.0)	0.259 (T6.5/T6.5)	0.278 (T6.5/T6.0)	...	0.298	0.137	T6.0	T6.5	T6.0
2M 1546-3325	...	0.316 (T6.0/T6.0)	0.303 (T6.0/T6.0)	0.302 (T6.0/T6.0)	...	0.367	0.152	T6.0	T6.0	T6.0
2M 2228-4310	...	0.305 (T6.0/T6.0)	0.261 (T6.5/T6.5)	0.228 (T6.5/T6.5)	0.061 (T7.0/-)	0.337	0.149	T6.0	T6.5	T6.5
2M 2356-1553	...	0.333 (T5.5/T6.0)	0.309 (T6.0/T5.5)	0.272 (T6.5/T6.5)	...	0.398	0.182	T6.0	T6.0	T6.0
SD 1624+0029	...	0.277 (T6.5/T6.5)	0.150 (T8.0/T8.0)	0.175 (T7.0/T7.5)	...	0.319	0.102	T6.0	T7.0	T7.5:
2M 0243-2453	...	0.278 (T6.5/T6.5)	0.270 (T6.5/T6.5)	0.254 (T6.5/T6.5)	0.139 (T6.0/T6.5)	0.390	0.143	T6.0	T6.5	T6.5
2M 0516-0445	...	0.307 (T6.0/T6.0)	0.309 (T6.0/T5.5)	0.214 (T6.5/T7.0)	0.173 (T5.5/T5.5)	0.393	0.255	T6.0	T6.0	T6.0
2M 2228-4310	...	0.305 (T6.0/T6.0)	0.261 (T6.5/T6.5)	0.228 (T6.5/T6.5)	0.061 (T7.0/-)	0.337	0.149	T6.0	T6.5	T6.5
2M 0727+1710	...	0.331 (T5.5/T6.0)	0.214 (T7.0/T7.5)	0.138 (T7.5/T7.5)	0.142	T7.0	T6.5:	T7.0
2M 1553+1532	...	0.190 (T8.0/T8.0)	0.212 (T7.5/T7.5)	0.132 (T8.0/T7.5)	...	0.428	0.101	T7.0	T8.0	T7.5
2M 0348-6022	...	0.245 (T7.0/T7.0)	0.192 (T8.0/T7.5)	0.173 (T7.0/T7.5)	0.116 (T6.5/-)	0.282	0.205	T7.0	T7.0	T7.5
Gl 570D	...	0.168 (T8.0/T8.0)	0.206 (T7.5/T7.5)	0.117 (T8.0/T8.0)	...	0.349	0.116	T7.5	T8.0	T8.0
2M 0415-0935	...	0.148 (T8.0/T8.0)	0.174 (T8.0/T8.0)	0.085 (T8.0/T8.0)	...	0.372	0.130	T8.0	T8.0	T8.0

Note. — Index subtypes in parentheses determined by direct comparison to spectral standard ratios (Table 4) or spectral ratio ranges (Table 5); see § 4.2.2. Uncertain classifications are indicated by “:”; peculiar sources are indicated by “p”.

Table 12. Spectral Indices and Classifications for Other Published Spectra.

Name (1)	H ₂ O-J (2)	CH ₄ -J (3)	H ₂ O-H (4)	CH ₄ -H (5)	CH ₄ -K (6)	H ₂ O-K (7)	K/J (8)	Derived NIR SpT			Ref (12)
								Direct (9)	Ind 1 (10)	Ind 2 (11)	
2M 0920+3517	...	0.739 (L9.0/T0.5)	...	0.867 (T2.0/T2.0)	0.901 (L8.0/-)	0.657	0.610	T0.0p	L9.5:	T1.5:	1
ϵ Indi Ba	0.593 (T0.5/T0.5)	0.904 (T1.5/T1.5)	T1.0	T1.0	T1.0	2
SD 1254-0122	0.491 (T2.0/T2.0)	0.560 (T2.0/T3.0)	0.507 (T2.0/T2.0)	0.846 (T2.0/T2.0)	0.564 (T2.0/T2.5)	0.549	0.354	T2.0	T2.0	T2.5	3
IFA 0230-Z1	0.646 (T3.5/T3.5)	T3.0:	T3.5:	T3.5:	4
SD 1750+1759	0.471 (T2.5/T2.5)	0.507 (T3.5/T4.0)	0.475 (T2.5/T2.5)	0.605 (T3.5/T3.5)	0.416 (T3.5/T3.0)	0.602	0.176	T3.5	T3.0	T3.0	3
2M 0559-1404	0.333 (T4.5/T4.5)	0.451 (T4.5/T4.5)	0.426 (T4.0/T3.5)	0.490 (T4.5/T4.5)	0.256 (T4.5/T4.5)	0.627	0.173	T4.5	T4.5	T4.5	5
ϵ Indi Bb	0.345 (T5.0/T5.0)	0.306 (T6.0/T6.0)	T6.0	T5.5	T5.5	2
NT 1205-0744	0.112 (T6.5/T7.0)	0.326 (T6.0/T6.0)	0.140 (T8.0/T8.0)	0.244 (T6.5/T6.5)	0.240 (T4.5/T4.5)	0.376	0.159	T7.0	T6.5:	T6.5:	6
2M 1217-0311	0.067 (T7.5/T7.5)	0.201 (T8.0/T7.5)	0.223 (T7.0/T7.0)	0.129 (T8.0/T8.0)	0.092 (T6.5/-)	0.359	0.171	T7.5	T7.5	T7.5	3

Note. — Index subtypes in parentheses determined by direct comparison to spectral standard ratios (Table 4) or spectral ratio ranges (Table 5); see § 4.2.2. Uncertain classifications are indicated by “:”; peculiar sources are indicated by “p”.

References. — (1) Nakajima et al. (2001); (2) McCaughrean et al. (2004); (3) Nakajima et al. (2004); (4) Liu et al. (2002); (5) Burgasser et al. (2000c); (6) Cuby et al. (1999)

Table 13. Comparison of T Dwarf Spectral Types

Object (1)	NIR Spectral Type		
	New (2)	B02 (3)	G02 (4)
SDSS 2047-0718	T0.0:	...	L9.5±1
SDSS 1104+5548	T0.0:	...	L9.5±1.5
SDSS 1207+0244	T0.0	...	T0
SDSS 1516+0259	T0.0:	...	T0±1.5
SDSS 0423-0414	T0.0	T0 ^a	T0
SDSS 0151+1244	T0.5	T0.5	T1±1
SDSS 0837-0000	T1.0	T1	T0.5
ε Indi Ba	T1.0	T1	T0.5
SDSS 1632+4150	T1.0:	...	T1±1
SDSS 1157+0611	T1.5	...	T1.5
2MASS 0949-1545	T2.0	T1 ^a	...
SDSS 1750+4222	T2.0	...	T1
2MASS 1122-3512	T2.0	T2 ^a	...
SDSS 0758+3247	T2.0	...	T2±1
SDSS 1521+0131	T2.0:	...	T2
SDSS 1254-0122	T2.0	T2	T2
2MASS 1209-1004	T3.0	T3 ^a	...
SDSS 1021-0304	T3.0	T3	T3
SDSS 1750+1759	T3.5	T3.5 ^a	T3.5
2MASS 2151-4853	T4.0	T4.5 ^a	...
2MASS 2254+3123	T4.0	T5	T4
SDSS 0000+2554	T4.5	...	T4.5
SDSS 0207+0000	T4.5	...	T4.5
SDSS 0926+5847	T4.5	...	T4.5
2MASS 0559-1404	T4.5	T5	T4.5
SDSS 0830+0128	T4.5	...	T5.5
2MASS 0755+2212	T5.0	T5:	...
2MASS 1901+4718	T5.0	T5 ^a	...
2MASS 2331-4718	T5.0	T5 ^a	...
SDSS 0742+2053	T5.0	...	T5
2MASS 0407+1514	T5.0	T5.5 ^a	...
2MASS 1503+2525	T5.0	T5.5	...
SDSS 0741+2351	T5.0	...	T5.5
2MASS 2339+1352	T5.0	T5.5	T5.5
2MASS 1828-4849	T5.0	T6 ^a	...
2MASS 2356-1553	T5.0	T6	...
SDSS 2124+0059	T5.0	...	T6
SDSS 1110+0116	T5.5	...	T5.5
2MASS 1231+0847	T5.5	T6 ^a	T5.5
ε Indi Bb	T6.0	T5.5	T5±1
2MASS 0516-0445	T6.0	T5.5	...
2MASS 0243-2453	T6.0	T6	...
2MASS 1225-2739	T6.0	T6	T6

Table 13—Continued

Object (1)	NIR Spectral Type		
	New (2)	B02 (3)	G02 (4)
SDSS 1624+0029	T6.0	T6	T6
2MASS 0937+2931	T6.0p	T6p	T6
2MASS 2228-4310	T6.0	T6.5	...
SDSS 1346-0031	T6.5	T6	T6
2MASS 1237+6526	T6.5	T6.5	...
2MASS 1047+2124	T6.5	T6.5	T6.5
2MASS 0034+0523	T6.5	T7	...
SDSS 1758+4633	T6.5	...	T7
NTTDF 1205-0744	T7.0:	T6:	...
Gliese 229B	T7.0p	T6.5	T6±1
2MASS 0348-6022	T7.0	T7	...
2MASS 0727+1710	T7.0	T7	T8
2MASS 0050-3322	T7.0	T7.5 ^a	...
2MASS 1114-2618	T7.5	T7.5 ^a	...
2MASS 1217-0311	T7.5	T7.5	T8
Gliese 570D	T7.5	T8	T8
2MASS 0939-2448	T8.0	T8 ^a	...
2MASS 0415-0935	T8.0	T8	T9

^aBased on revised indices similar to Table 3 (Burgasser et al. 2004a; Tinney et al. 2005).

Table 14. T Dwarf Compendium

Name	NIR SpT ^d	J2000 Coordinates ^a			SDSS ^b <i>z</i>	2MASS ^c			π (mas)	μ ($''$ yr ⁻¹)	ϕ ($^{\circ}$)	Ref ^e
		α	δ	Epoch		<i>J</i> (mag)	<i>H</i> (mag)	<i>K_s</i> (mag)				
(1)	(2)	(3)	(4)	(5)	(6)	(7)	(8)	(9)	(10)	(11)	(12)	(13)
SDSS J000013.54+255418.6	T4.5	00 ^h 00 ^m 13 ^s .54	+25°54′18″.0	1998.76	18.48±0.04	15.06±0.04	14.73±0.07	14.84±0.12	1
2MASS J00345157+0523050	T6.5	00 ^h 34 ^m 51 ^s .57	+05°23′05″.0	2000.67	...	15.54±0.05	15.44±0.08	> 16.2	...	0.68±0.06	72	2
2MASS J00501994-3322402	T7	00 ^h 50 ^m 19 ^s .94	-33°22′40″.2	1998.87	...	15.93±0.07	15.84±0.19	15.24±0.19	...	1.5±0.1	307	3
SDSS J015141.69+124429.6	T0.5	01 ^h 51 ^m 41 ^s .55	+12°44′30″.0	1997.70	19.40±0.07	16.57±0.13	15.60±0.11	15.18±0.19	47±3	0.743±0.004	93	4,24
SDSS J020742.48+000056.2	T4.5	02 ^h 07 ^m 42 ^s .84	+00°00′56″.4	2000.63	20.08±0.12	16.63±0.05 ^f	16.66±0.05 ^f	16.62±0.05 ^f	35±10	0.156±0.011	96	4,24,25
Ifa 0230-Z1	T3	02 ^h 26 ^m 37 ^s .60	+00°51′54″.7	2000.81	...	18.17±0.03 ^g	17.83±0.04 ^g	5
2MASS J02431371-2453298	T6	02 ^h 43 ^m 13 ^s .71	-24°53′29″.8	1998.86	...	15.38±0.05	15.14±0.11	15.22±0.17	94±4	0.355±0.004	234	6,24
2MASS J03480772-6022270	T7	03 ^h 48 ^m 07 ^s .72	-60°22′27″.0	1999.88	...	15.32±0.05	15.56±0.14	15.60±0.23	...	0.77±0.04	201	7
2MASS J04070885+1514565	T5	04 ^h 07 ^m 08 ^s .85	+15°14′56″.5	1999.90	...	16.06±0.09	16.02±0.21	15.92±0.26	2
2MASS J04151954-0935066	T8	04 ^h 15 ^m 19 ^s .54	-09°35′06″.6	1998.87	...	15.70±0.06	15.54±0.11	15.43±0.20	174±3	2.255±0.003	76	6,24
SDSS J042348.57-041403.5AB	T0	04 ^h 23 ^m 48 ^s .58	-04°14′03″.5	1998.73	17.33±0.03	14.47±0.03	13.46±0.04	12.93±0.03	65.9±1.7	0.333±0.003	284	4,24,27
2MASS J05160945-0445499	T5.5	05 ^h 16 ^m 09 ^s .45	-04°45′49″.9	1998.72	...	15.98±0.08	15.72±0.17	15.49±0.20	...	0.34±0.03	232	7
2MASS J05185995-2828372	T1p	05 ^h 18 ^m 59 ^s .95	-28°28′37″.2	1999.01	...	15.98±0.10	14.83±0.07	14.16±0.07	8
S Ori 70	T6:	05 ^h 38 ^m 10 ^s .1	-02°36′26″	2000.85	...	20.28±0.10 ^h	20.42±0.11 ^h	19.78±0.17 ^h	9,28
2MASS J05591914-1404488	T4.5	05 ^h 59 ^m 19 ^s .14	-14°04′48″.8	1998.95	...	13.80±0.02	13.68±0.04	13.58±0.05	97.7±1.3	0.6612±0.0012	122	10,29
Gliese 229B	T7p	06 ^h 10 ^m 34 ^s .74 ⁱ	-21°51′59″.5 ⁱ	1999.03	...	14.32±0.05 ^j	14.35±0.05 ^j	14.42±0.05 ^j	173.2±1.1	0.727±0.005	191	11,26,30,31
2MASS J07271824+1710012	T7	07 ^h 27 ^m 18 ^s .24	+17°10′01″.2	1997.83	...	15.60±0.06	15.76±0.17	15.56±0.19	110±2	1.297±0.005	126	6,24
SDSS J074149.15+235127.5	T5	07 ^h 41 ^m 49 ^s .20	+23°51′27″.5	1997.92	19.47±0.08	16.16±0.10	15.84±0.19	> 15.9	1
SDSS J074201.41+205520.5	T5	07 ^h 42 ^m 01 ^s .30	+20°55′19″.8	1997.92	19.47±0.09	16.19±0.09	15.91±0.18	> 15.2	1
2MASS J07554795+2212169	T5	07 ^h 55 ^m 47 ^s .95	+22°12′16″.9	1998.82	18.41±0.06	15.73±0.06	15.67±0.15	15.75±0.21	6
SDSS J075840.33+324723.4	T2	07 ^h 58 ^m 40 ^s .37	+32°47′24″.5	1998.34	17.97±0.02	14.95±0.04	14.11±0.04	13.88±0.06	1
SDSS J083048.80+012831.1	T4.5	08 ^h 30 ^m 48 ^s .78	+01°28′31″.1	2000.08	19.59±0.08	16.29±0.11	16.14±0.21	> 16.4	1
SDSS J083717.22-000018.3	T1	08 ^h 37 ^m 17 ^s .21	-00°00′18″.0	1999.22	19.83±0.10	16.90±0.05 ^f	16.21±0.05 ^f	15.98±0.05 ^f	34±14	0.173±0.017	185	12,24
Gliese 377CD	T0	09 ^h 12 ^m 14 ^s .69	+14°59′39″.6	1997.88	...	15.51±0.08	14.62±0.08	14.04±0.06	48.8±0.9	0.5789±0.0014	295	13,26,32,33
2MASS J09201223+3517429AB	TOp	09 ^h 20 ^m 12 ^s .23	+35°17′42″.9	1998.23	18.27±0.04	15.63±0.06	14.67±0.06	13.98±0.06	14,35
SDSS J092615.38+584720.9AB	T4.5	09 ^h 26 ^m 15 ^s .37	+58°47′21″.2	2000.22	19.03±0.06	15.90±0.07	15.31±0.10	15.45±0.19	...	< 0.3	...	4,19,36
2MASS J09373487+2931409	T6p	09 ^h 37 ^m 34 ^s .87	+29°31′40″.9	2000.25	...	14.65±0.04	14.70±0.07	15.27±0.13	163±4	1.622±0.007	143	6,24
2MASS J09393548-2448279	T8	09 ^h 39 ^m 35 ^s .48	-24°48′27″.9	2000.11	...	15.98±0.11	15.80±0.15	> 16.6	...	1.15±0.06	155	3
2MASS J09490860-1545485	T2	09 ^h 49 ^m 08 ^s .60	-15°45′48″.5	2000.19	...	16.15±0.12	15.26±0.11	15.23±0.17	...	0.10±0.04	271	3
SDSS J102109.69-030420.1AB	T3	10 ^h 21 ^m 09 ^s .69	-03°04′19″.7	1998.93	19.28±0.05	16.25±0.09	15.35±0.10	15.13±0.17	34±5	0.183±0.003	249	12,36,37
2MASS J10475385+2124234	T6.5	10 ^h 47 ^m 53 ^s .85	+21°24′23″.4	1998.08	...	15.82±0.06	15.80±0.12	> 16.4	95±4	1.728±0.008	254	15,24
SDSS J110454.24+554841.3	T0:	11 ^h 04 ^m 54 ^s .25	+55°48′41″.4	2001.89	19.94±0.10	17.31±0.05 ^f	16.71±0.05 ^f	16.31±0.05 ^f	1
SDSS J111010.01+011613.1	T5.5	11 ^h 10 ^m 10 ^s .01	+01°16′13″.0	2000.12	19.68±0.11	16.34±0.12	15.92±0.14	> 15.1	...	0.34±0.10	110	4,1,3
2MASS J11145133-2618235	T7.5	11 ^h 14 ^m 51 ^s .33	-26°18′23″.5	1999.19	...	15.86±0.08	15.73±0.12	> 16.1	...	3.05±0.04	263	3
2MASS J11220826-3512363	T2	11 ^h 22 ^m 08 ^s .26	-35°12′36″.3	1999.23	...	15.02±0.04	14.36±0.05	14.38±0.07	...	0.29±0.03	211	3
SDSS J115700.50+061105.2	T1.5	11 ^h 57 ^m 00 ^s .50	+06°11′05″.2	2001.45	20.21±0.11	17.09±0.05 ^f	16.45±0.05 ^f	16.00±0.05 ^f	1
NTTDF 1205-0744	T6:	12 ^h 05 ^m 20 ^s .21	-07°44′01″.0	1997.16	...	20.15 ^k	...	20.30 ^k	16
SDSS J120747.17+024424.8	T0	12 ^h 07 ^m 47 ^s .17	+02°44′24″.9	2000.13	18.39±0.04	15.58±0.07	14.56±0.07	13.99±0.06	...	0.39±0.09	286	1,3
2MASS J12095613-1004008	T3	12 ^h 09 ^m 56 ^s .13	-10°04′00″.8	1999.10	...	15.91±0.07	15.33±0.09	15.06±0.14	...	0.46±0.10	140	2
2MASS J12171110-0311131	T7.5	12 ^h 17 ^m 11 ^s .10	-03°11′13″.1	1999.08	19.36±0.07	15.86±0.06	15.75±0.12	> 15.9	91±2	1.0571±0.0017	274	15,37
2MASS J12255432-2739466AB	T6	12 ^h 25 ^m 54 ^s .32	-27°39′46″.6	1998.51	...	15.26±0.05	15.10±0.08	15.07±0.15	75±3	0.737±0.003	149	15,37,38
2MASS J12314753+0847331	T5.5	12 ^h 31 ^m 47 ^s .53	+08°47′33″.1	2000.21	18.94±0.04	15.57±0.07	15.31±0.11	15.22±0.20	...	1.61±0.07	227	1,2,3
2MASS J12373919+6526148	T6.5	12 ^h 37 ^m 39 ^s .19	+65°26′14″.8	1999.20	19.56±0.08	16.05±0.09	15.74±0.15	> 16.1	96±5	1.131±0.009	242	15,24
SDSS J125453.90-012247.4	T2	12 ^h 54 ^m 53 ^s .93	-01°22′47″.4	1999.06	18.00±0.03	14.89±0.04	14.09±0.03	13.84±0.05	73.2±1.9	0.491±0.003	285	12,37
SDSS J134646.45-003150.4	T6.5	13 ^h 46 ^m 46 ^s .34	-00°31′50″.1	2001.09	19.16±0.05	16.00±0.10	15.46±0.12	15.77±0.27	68±2	0.516±0.003	257	17,37
Gliese 570D	T7.5	14 ^h 57 ^m 14 ^s .96	-21°21′47″.7	1998.37	...	15.32±0.05	15.27±0.09	15.24±0.16	169.3±1.7	2.012±0.004	149	18,26
2MASS J15031961+2525196	T5	15 ^h 03 ^m 19 ^s .61	+25°25′19″.6	1999.39	17.292±0.014	13.94±0.02	13.86±0.03	13.96±0.06	19

Table 14—Continued

Name	NIR SpT ^d	J2000 Coordinates ^a			SDSS ^b <i>z</i>	2MASS ^c			π (marcs)	μ ($''$ yr ⁻¹)	ϕ ($^\circ$)	Ref ^e
		α	δ	Epoch		<i>J</i> (mag)	<i>H</i> (mag)	<i>K_s</i> (mag)				
(1)	(2)	(3)	(4)	(5)	(6)	(7)	(8)	(9)	(10)	(11)	(12)	(13)
SDSS J151603.03+025928.9	T0:	15 ^h 16 ^m 03 ^s .03	+02 [°] 59′29″.2	2000.31	19.60±0.08	17.23±0.20	16.00±0.15	15.43±0.18	1
SDSS J152103.24+013142.7	T2:	15 ^h 21 ^m 03 ^s .27	+01 [°] 31′42″.6	2000.31	19.57±0.06	16.40±0.10	15.58±0.10	15.35±0.17	1
2MASS J15344984−2952274AB	T5.5	15 ^h 34 ^m 49 ^s .84	−29 [°] 52′27″.4	1998.52	...	14.90±0.05	14.87±0.10	14.84±0.11	73.6±1.2	0.2688±0.0019	159	6,37,38
2MASS J15462718−3325111	T5.5	15 ^h 46 ^m 27 ^s .18	−33 [°] 25′11″.1	1998.52	...	15.63±0.05	15.45±0.09	15.49±0.18	88.0±1.9	0.225±0.002	33	6,37
2MASS J15530228+1532369AB	T7	15 ^h 53 ^m 02 ^s .28	+15 [°] 32′36″.9	1998.14	...	15.83±0.07	15.94±0.16	15.51±0.18	6,36
SDSS J162414.37+002915.6	T6	16 ^h 24 ^m 14 ^s .36	+00 [°] 29′15″.8	1999.31	19.05±0.04	15.49±0.05	15.52±0.10	> 15.5	92±2	0.3832±0.0019	270	20,29
SDSS J163239.34+415004.3	T1:	16 ^h 32 ^m 39 ^s .34	+41 [°] 50′04″.3	2001.39	20.35±0.11	16.87±0.05 ^f	16.42±0.05 ^f	16.19±0.05 ^f	1
SDSS J175024.01+422237.8	T2	17 ^h 50 ^m 23 ^s .85	+42 [°] 22′37″.3	1998.44	19.38±0.09	16.47±0.10	15.42±0.09	15.48±0.17	1
SDSS J175032.96+175903.9	T3.5	17 ^h 50 ^m 32 ^s .93	+17 [°] 59′04″.2	1999.23	19.63±0.06	16.34±0.10	15.95±0.13	15.48±0.19	36±5	0.204±0.008	61	4,24
SDSS J175805.46+463311.9	T6.5	17 ^h 58 ^m 05 ^s .45	+46 [°] 33′09″.9	1998.44	19.67±0.07	16.15±0.09	16.25±0.22	15.47±0.19	1
2MASS J18283572−4849046	T5.5	18 ^h 28 ^m 35 ^s .72	−48 [°] 49′04″.6	2000.77	...	15.18±0.06	14.91±0.07	15.18±0.14	...	0.34±0.06	84	2,3
2MASS J19010601+4718136	T5	19 ^h 01 ^m 06 ^s .01	+47 [°] 18′13″.6	1998.47	...	15.86±0.07	15.47±0.09	15.64±0.29	...	0.38±0.22	17	2
SDSS J204749.61−071818.3	T0:	20 ^h 47 ^m 49 ^s .61	−07 [°] 18′18″.3	2000.74	19.70±0.10	16.70±0.03 ^f	15.88±0.03 ^f	15.34±0.03 ^f	1
SDSS J212413.89+010000.3	T5	21 ^h 24 ^m 13 ^s .87	+00 [°] 59′59″.9	2000.63	19.74±0.09	16.03±0.07	16.18±0.20	> 16.1	1
2MASS J21392676+0220226	T1.5	21 ^h 39 ^m 26 ^s .76	+02 [°] 20′22″.6	2000.54	...	15.26±0.05	14.17±0.05	13.58±0.05	21
2MASS J21513839−4853542	T4	21 ^h 51 ^m 38 ^s .39	−48 [°] 53′54″.2	1999.72	...	15.73±0.07	15.17±0.10	15.43±0.18	...	0.57±0.07	113	22
Eps Ind Bab	T1/T6 ^l	22 ^h 04 ^m 10 ^s .52	−56 [°] 46′57″.7	1999.85	...	11.91±0.02	11.31±0.02	11.21±0.02	275.8±0.7	4.7049±0.0010	327	23,26,39
2MASS J22282889−4310262	T6	22 ^h 28 ^m 28 ^s .89	−43 [°] 10′26″.2	1998.89	...	15.66±0.07	15.36±0.12	15.30±0.21	...	0.31±0.03	175	7
2MASS J22541892+3123498	T4	22 ^h 54 ^m 18 ^s .92	+31 [°] 23′49″.8	1998.47	...	15.26±0.05	15.02±0.08	14.90±0.15	6
2MASS J23312378−4718274	T5	23 ^h 31 ^m 23 ^s .78	−47 [°] 18′27″.4	2000.79	...	15.66±0.07	15.51±0.15	15.39±0.20	...	0.20±0.07	118	2,37
2MASS J23391025+1352284	T5	23 ^h 39 ^m 10 ^s .25	+13 [°] 52′28″.4	2000.91	19.42±0.07	16.24±0.11	15.82±0.15	16.15±0.31	...	0.83±0.11	159	6,19
2MASS J23565477−1553111	T5.5	23 ^h 56 ^m 54 ^s .77	−15 [°] 53′11″.1	1998.54	...	15.82±0.06	15.63±0.10	15.77±0.18	69±3	0.746±0.003	216	6,24

^aIf detected in 2MASS, coordinates are from the 2MASS All Sky Point Source Catalog (Cutri et al. 2003), epoch \sim 1997-2001; otherwise coordinates are from discovery reference.

^bSDSS *z* AB magnitudes from SDSS Data Release 4 (Adelman-McCarthy et al. 2005) or the literature (Leggett et al. 2000; Geballe et al. 2002; Knapp et al. 2004).

^cUnless otherwise noted.

^dNear infrared spectral type on unified scheme; see § 4.

^eDiscovery reference in boldface type, followed by references for additional photometric and astrometric data.

^fMKO *JHK* from Leggett et al. (2002b) or Knapp et al. (2004).

^gMKO *JH* photometry from Liu et al. (2002).

^h*JHK* photometry from Zapatero Osorio et al. (2002).

ⁱCoordinates for Gliese 229B determined from 2MASS coordinates of Gliese 229A and offsets from Golimowski et al. (1998).

^jUKIRT *JHK* photometry from Leggett et al. (1999).

^k*JK* photometry from Cuby et al. (1999).

^lSpectral types from resolved spectroscopy (see Table 12).

References. — (1) Knapp et al. (2004); (2) Burgasser et al. (2004a); (3) Tinney et al. (2005); (4) G02; (5) Liu et al. (2002); (6) B02; (7) Burgasser, McElwain, & Kirkpatrick (2003); (8) Cruz et al. (2004); (9) Zapatero Osorio et al. (2002); (10) Burgasser et al. (2000c); (11) Nakajima et al. (1995); (12) Leggett et al. (2000); (13) Wilson et al. (2001b); (14) Kirkpatrick et al. (2000); (15) Burgasser et al. (1999); (16) Cuby et al. (1999); (17) Tsvetanov et al. (2000); (18) Burgasser et al. (2000b);

(19) Burgasser et al. (2003c); (20) Strauss et al. (1999); (21) Cruz et al. in prep.; (22) Ellis et al. (2005); (23) Scholz et al. (2003); (24) Vrba et al. (2004); (25) Leggett et al. (2002b); (26) HIPPARCOS (ESA 1997); (27) Burgasser et al. (2005); (28) Martín & Zapatero Osorio (2003); (29) Dahn et al. (2002); (30) Oppenheimer et al. (1995); (31) Leggett et al. (1999); (32) McLean et al. (2003); (33) Burgasser, Kirkpatrick & Lowrance (2005); (34) Nakajima et al. (2001); (35) Reid et al. (2001); (36) Burgasser et al., in prep.; (37) Tinney, Burgasser, & Kirkpatrick (2003); (38) Burgasser et al. (2003d); (39) McCaughrean et al. (2004)

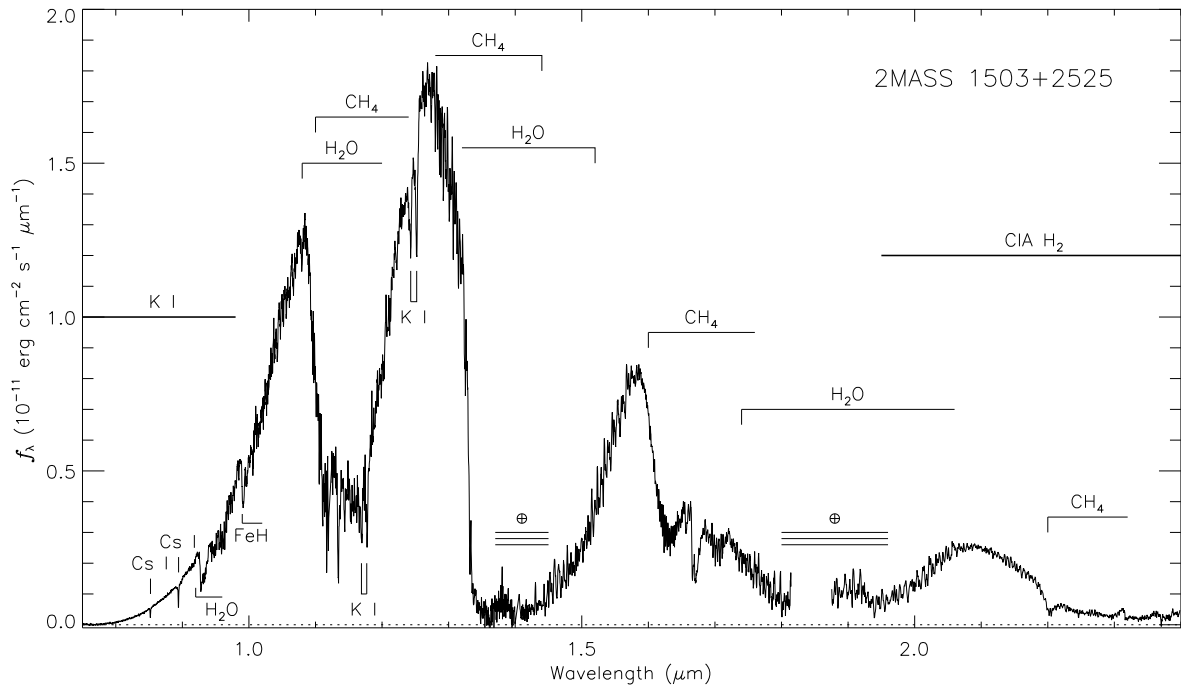


Fig. 1.— The 0.75–2.5 μm spectrum of the T5 spectral standard 2MASS 1503+2525 observed at a spectral resolution $\lambda/\Delta\lambda\sim 1200$ (Burgasser et al. 2003b, 2004a). Defining features of T dwarf near infrared spectra are labelled.

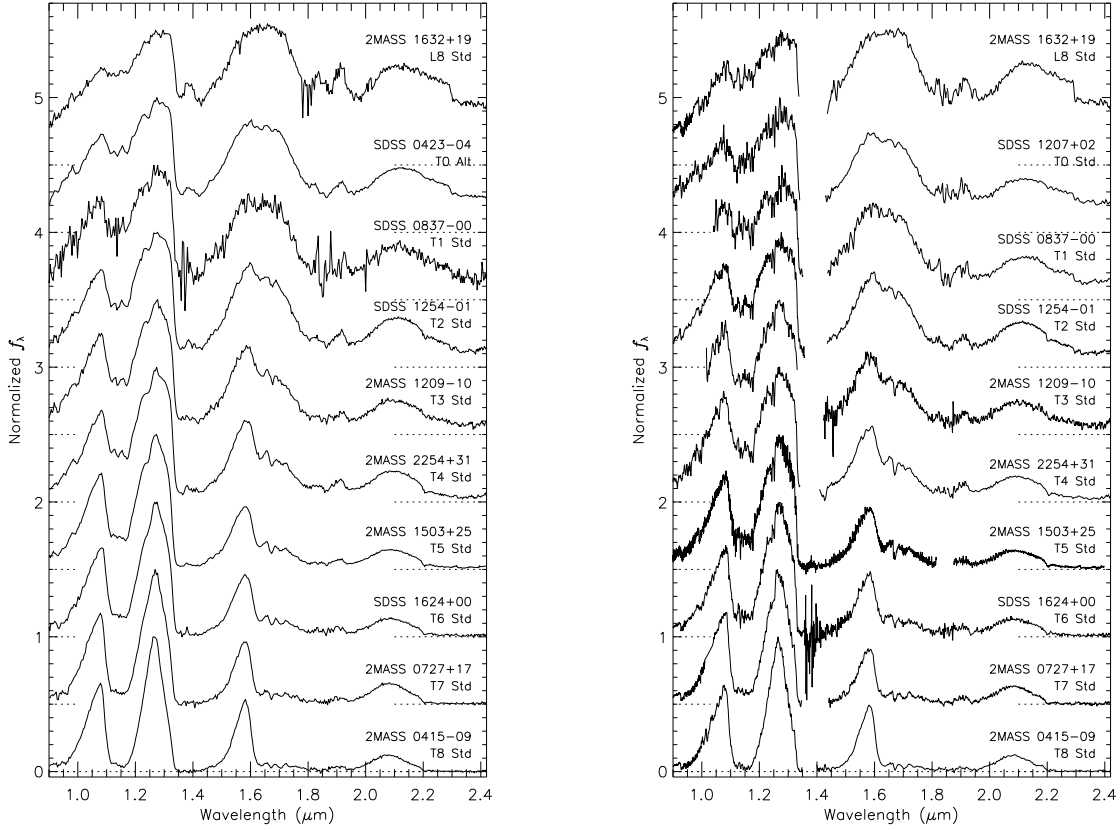


Fig. 2.— Near infrared spectra of T dwarf standards, along with the L8 optical standard 2MASS 1632+1904 (Kirkpatrick et al. 1999). Left panel displays the low resolution SpeX sample (note the substitution of the alternate T0 standard SDSS 0423–0414AB), right panel displays the moderate resolution CGS4 sample (with SpeX cross dispersed data for 2MASS 1503+2525). All spectra are normalized at $1.25 \mu\text{m}$ and offset by a constant (dotted lines).

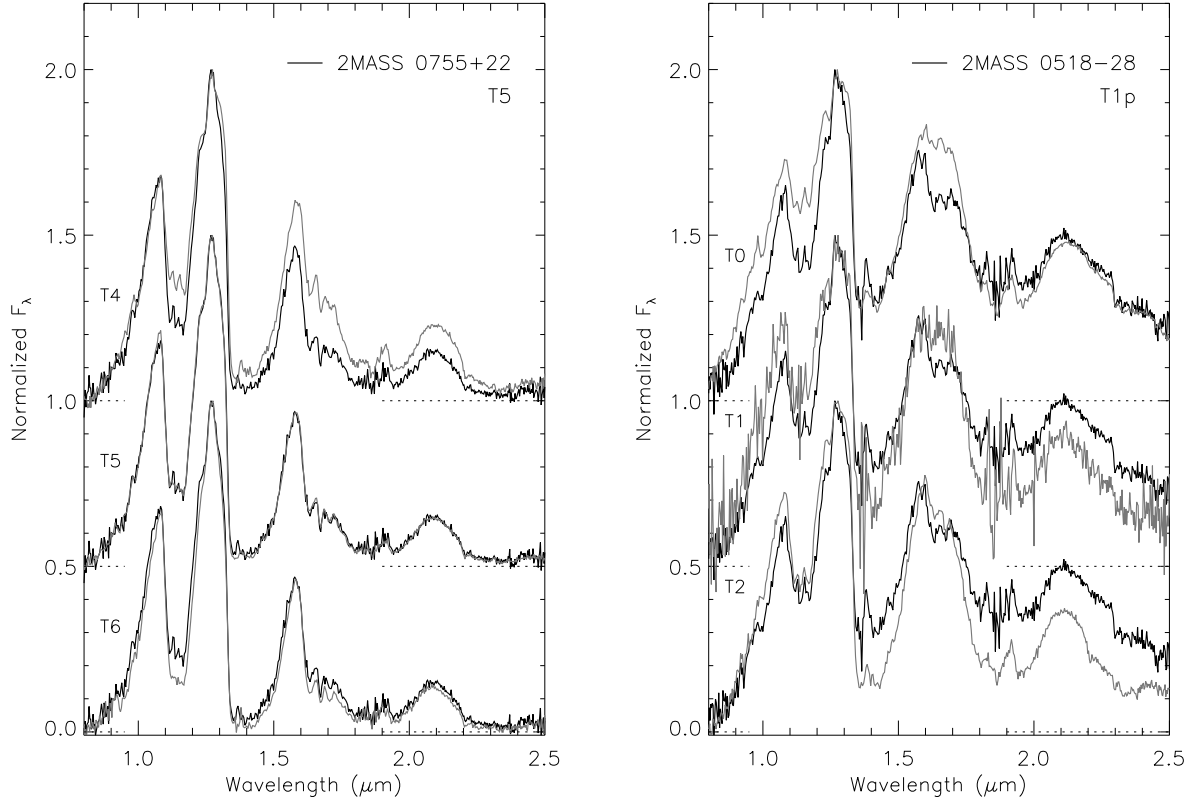


Fig. 3.— Examples of direct spectral classification for the low resolution SpeX data. The left panel demonstrates the case of the T5 2MASS 0755+2212 (B02), which closely matches the T5 standard 2MASS 1503+2525. The right panel demonstrates the case of the peculiar T1 2MASS 0518-2828 (Cruz et al. 2004), the spectrum of which does not match any of the T dwarf standards. This source is suspected to be an unresolved L dwarf/T dwarf binary. In both panels, source (black) and standard (grey) spectra are normalized at their J -band flux peaks and offset by constants (dotted lines).

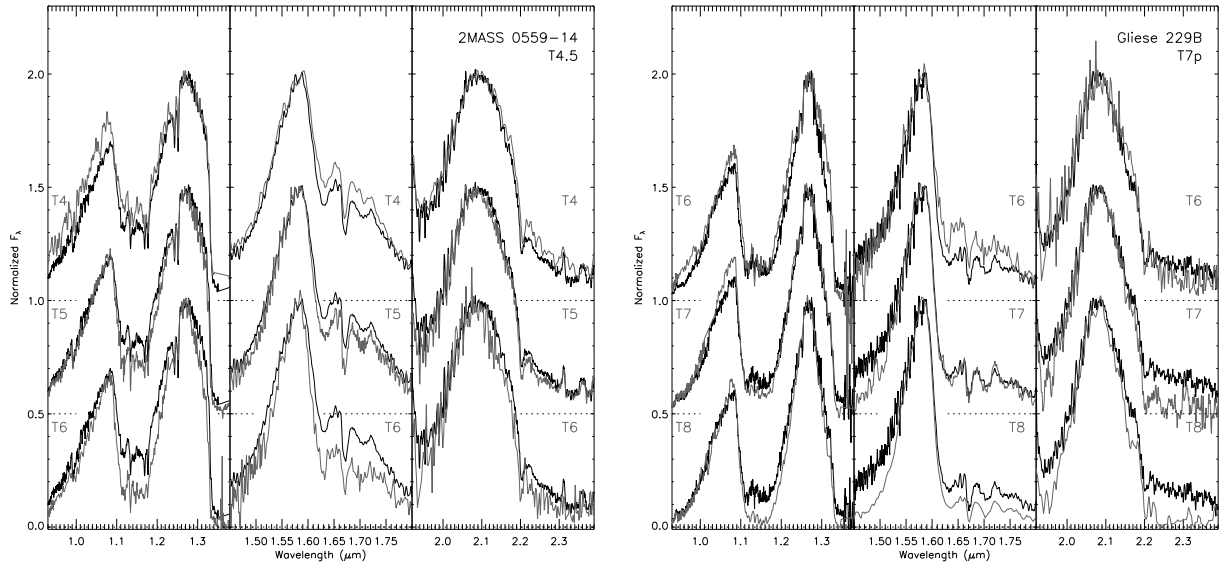


Fig. 4.— Similar to Figure 3 for moderate resolution CGS4 data. Here we show the examples of the T4.5 2MASS 0559–1404 and the peculiar T7 Gliese 229B. Spectral data are separated into three bands, with the source (black) and standard (grey) spectra normalized at their flux peaks within the band. Note how the features in the spectrum of 2MASS 0559–1404 fall midway in strength between the T4 and T5 standard; while the spectrum of Gliese 229B is inconsistent with any of the standards in all three spectral regions simultaneously.

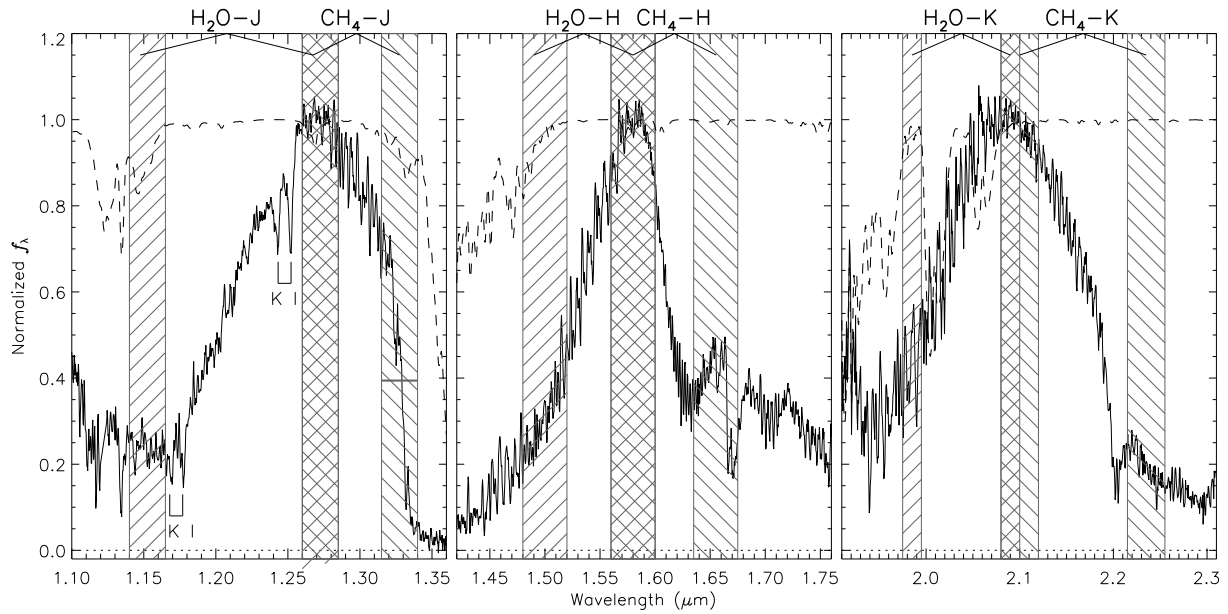


Fig. 5.— Spectral regions sampled by the six H_2O and CH_4 indices defined in Table 3, plotted on the near infrared spectrum of the T5 standard 2MASS 1503+2525 (Burgasser et al. 2004a). Not shown are the regions sampled by the K/J index. A telluric transmission spectrum typical for Mauna Kea is also shown (dashed lines) to highlight regions of low terrestrial atmospheric absorption. Spectral data in each panel are normalized at the local flux peak.

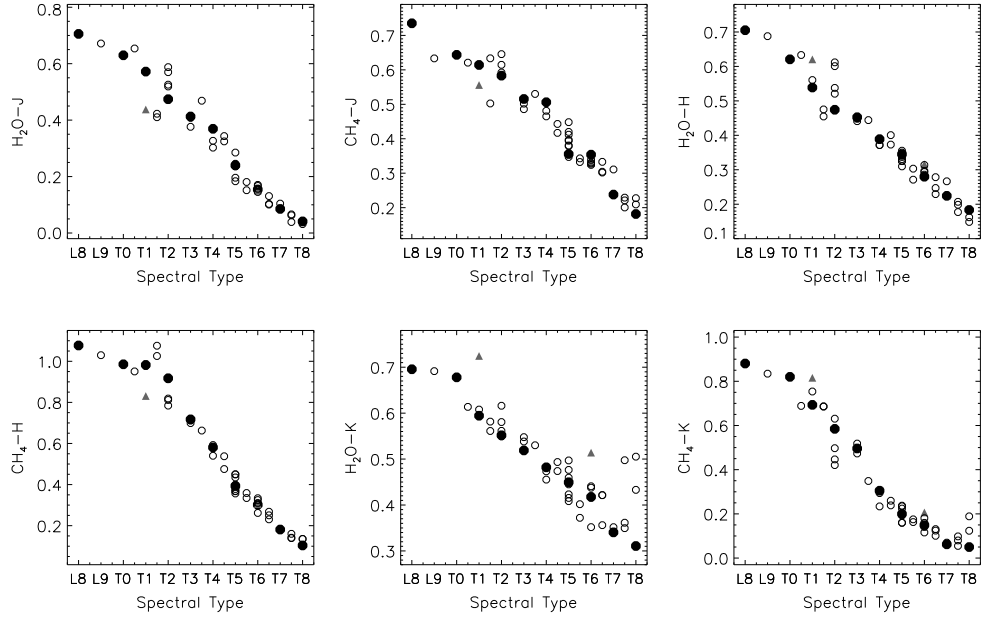


Fig. 6.— Values for the H_2O and CH_4 spectral indices measured on the SpeX prism data as a function of spectral type (as determined by direct spectral comparison). Primary standards are indicated by solid black circles, peculiar sources and uncertain classifications by solid grey triangles, and all other sources by open circles. Note the variable vertical scale in each panel.

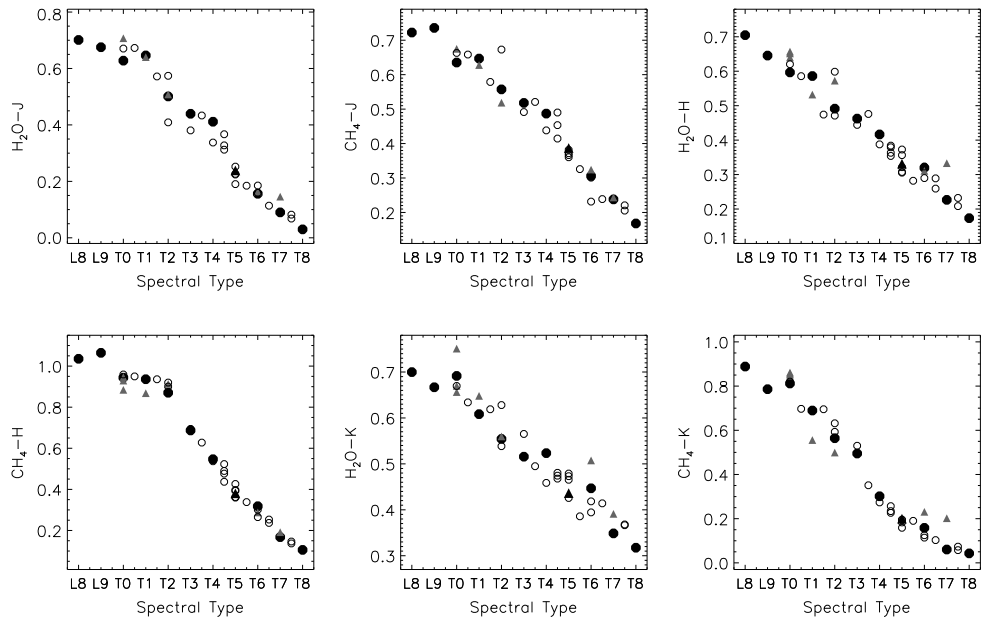


Fig. 7.— Same as Figure 6 for the CGS4 spectra.

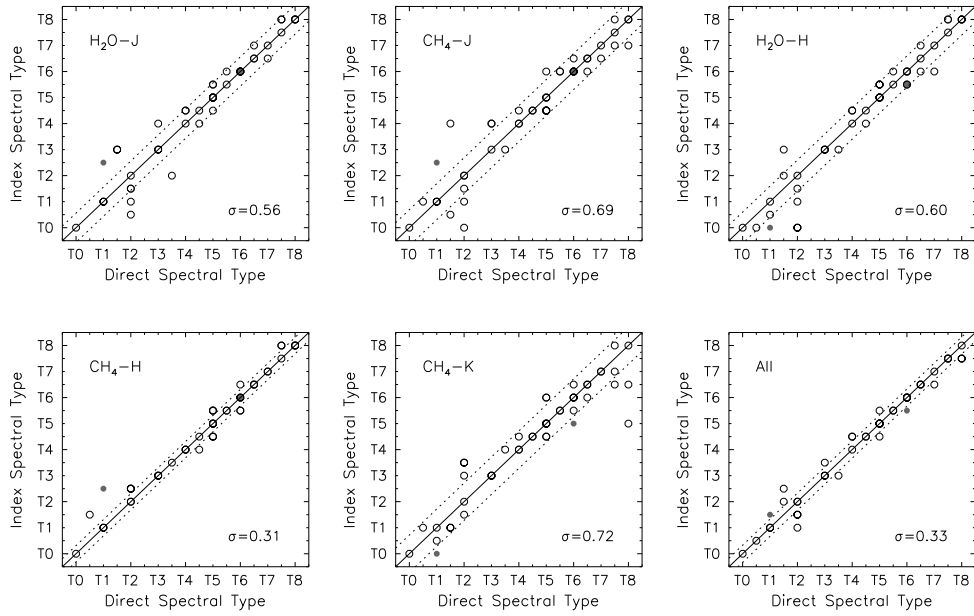


Fig. 8.— A comparison of index subtypes for the five primary classification indices, computed using the B02 method, versus subtypes determined by direct spectral comparison for the SpeX prism data. Peculiar T dwarfs and uncertain classifications are indicated by solid grey circles, all others by open circles. The solid line delineates perfect agreement between subtypes while the dotted lines indicate the $\pm 1\sigma$ scatter in subtype deviations, as listed in each panel.

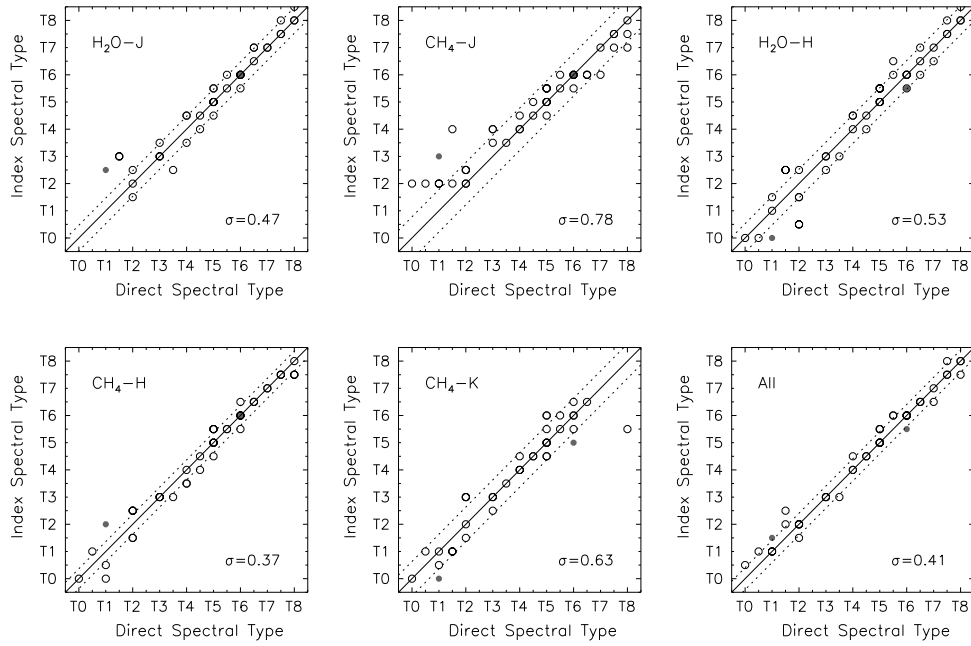


Fig. 9.— Same as Figure 8, but comparing index subtypes computed using the G02 method. Note the absence of data points where the index ranges (Table 3) are not defined.

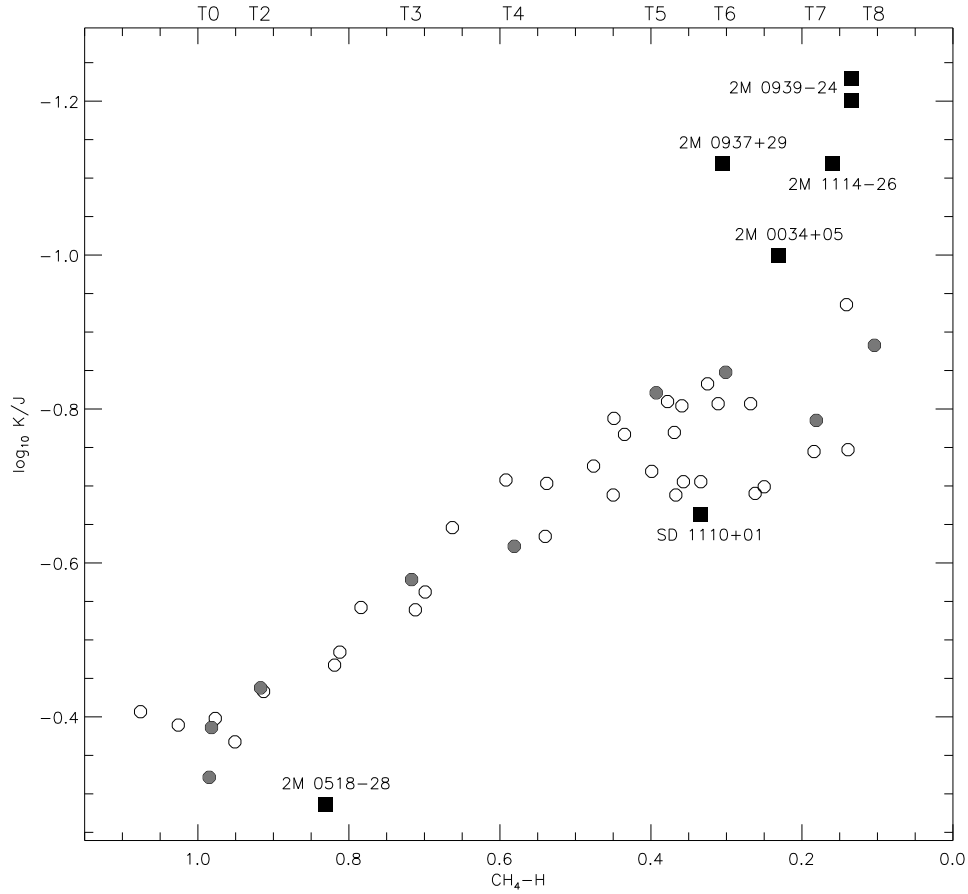


Fig. 10.— Comparison of K/J (on a logarithmic scale) and $\text{CH}_4\text{-H}$ indices as measured for SpeX prism data. Spectral standards are distinguished by grey circles. Sources suspected to have unusually high or low surface gravities or subsolar metallicities are indicated by black squares and labelled (2MASS 0518–2828 is separately discussed in § 6). The broad spread in the K/J indices amongst the late-type T dwarfs suggests that a second classification parameter may be required to fully describe their spectra.

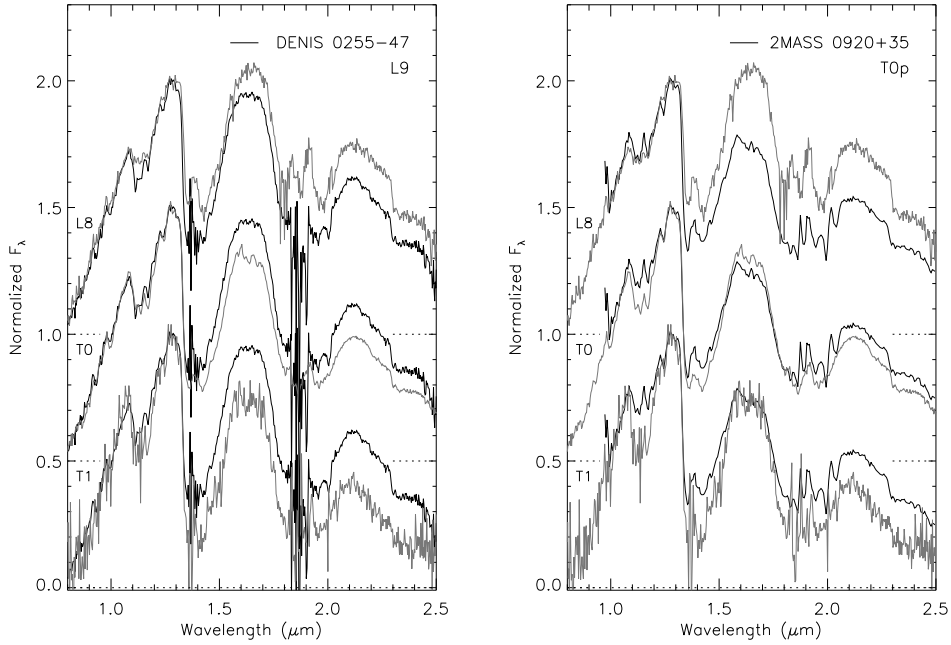


Fig. 11.— *Left*: Comparison of SpeX prism data for DENIS 0255–4700 (black line) to L8, T0 and T1 spectral standards (grey lines; note that the alternate standard SDSS 0423–0414AB is shown here). All of the spectra are normalized at their J -band flux peaks and offset by a constant (dotted lines). While Cushing, Rayner & Vacca (2005) have detected CH_4 absorption at $1.6 \mu\text{m}$ in a higher resolution SpeX spectrum of DENIS 0255–4700, this band is not seen in these low resolution data. *Right*: Similar comparison of NIRC grism data for 2MASS 0920+3517AB (B02). In this case CH_4 absorption at $1.6 \mu\text{m}$ is clearly present, although there are discrepancies in band strengths; e.g., the $\text{H}_2\text{O}/\text{CH}_4$ band at $1.1 \mu\text{m}$ as compared to the CH_4 band at $1.6 \mu\text{m}$. This source is therefore classified T0p in the near infrared, much later than its L6.5 optical classification (Kirkpatrick et al. 2000).